

Sedimentology and stable isotopes from a lacustrine-to-palustrine limestone deposited in an arid setting, climatic and tectonic factors: Miocene–Pliocene Opache Formation, Atacama Desert, Chile



Carol B. de Wet ^{a,*}, Linda Godfrey ^b, Andrew P. de Wet ^a

^a Department of Earth and Environment, Franklin & Marshall College, Lancaster, PA, USA

^b Department of Earth and Planetary Sciences, Rutgers University, Piscataway, NJ, USA

ARTICLE INFO

Article history:

Received 24 June 2014

Received in revised form 29 January 2015

Accepted 26 February 2015

Available online 5 March 2015

Keywords:

Atacama Desert

Lacustrine–palustrine limestone

Mio–Pliocene sea surface temperatures

ABSTRACT

Field relations, petrography, GIS, and geochemistry of a Late Miocene–Pliocene limestone, the Opache Formation, Calama Basin, Atacama Desert, Chile shows that depositional facies, diagenetic histories, and isotopes differ from eastern to western parts of the basin. We recognize two facies; lacustrine, characterized by ostracod-diatom mudstone and wackestone, and palustrine, characterized by both shallow water and pedogenic features. GIS analysis of the basin topography reveals an intrabasinal low in the eastern area and steeper hydrological gradients to the west, with the “Calama constriction”, restricting flow between east and west. Petrography and geochemical results confirm that the Calama constriction influenced depositional parameters, ponding groundwater to the east, forming a shallow lake and creating palustrine conditions to the west. Our analyses indicate that lake waters were less enriched in ^{13}C or ^{18}O than palustrine waters even though petrologic studies show that the lacustrine carbonates have a complex diagenetic history, derived from groundwater-rich in dissolved minerals. This seemingly contrary observation can be reconciled if an important source of water for the western carbonates was sourced from the Pacific Ocean and was less evolved, whereas eastern limestones precipitated from water which had become depleted in ^{18}O during transport from the east. Today, moisture from the Pacific very rarely, if ever, reaches inland as far as Calama, indicating that during the Late Miocene–Mid-Pliocene breakdown in the temperature inversion due to weakened or absent upwelling in the cold coastal Pacific current allowed moisture from the Pacific to reach inland. This changing atmospheric circulation pattern may have also affected upper level airflow that today blocks eastern sourced moisture from crossing the Andes, allowing it to reach farther westward into the Atacama region during the Late Miocene–Pliocene. Together, these moisture sources were sufficient to produce carbonate-rich palustrine and lacustrine environments in the Calama Basin.

© 2015 Elsevier B.V. All rights reserved.

1. Introduction

The deposition of sediments in closed and semi-closed basins is directly linked to climate and water budget (Cecil, 1990; Amundson et al., 2012). Sediments deposited in basins within the Atacama Desert of northern Chile during the latter part of the Cenozoic include siliciclastics, carbonate, diatomite and evaporite minerals, and many basins are characterized by gaps in their sedimentation history (Chong et al., 1999; May et al., 1999, 2005; Sáez et al., 1999; Pueyo et al., 2001; Pananont et al., 2004; Rech et al., 2006; Jordan et al., 2007; Nester et al., 2007; Blanco, 2008; Blanco and Tomlinson, 2009; Hartley and Evenstar, 2010). Sedimentation in the Atacama Desert is complex. Compared to temperate areas, small changes in the balance between precipitation and evaporation can change sedimentation style in the desert, either redistributing siliciclastic material after periods of negligible

sedimentation, allowing evaporite facies to develop, and in the case of the Calama Basin, resulting in the precipitation of large amounts of limestone. A second, and equally important factor is that the eastern edge of the Atacama Desert includes the flank of the Central Andes, a volcanically active arc that has seen over 3000 m of uplift over Neogene time. Volcanism and uplift can supply large amounts of detrital material on regional and local scales, which could overwhelm subtle changes in sedimentation caused by changes in climate. Distinguishing tectonic from climatic drivers of sedimentation is important.

Sedimentary successions within different basins adjacent to the western slope of the Andes deposited during the latter half of the Cenozoic are dominated by conglomerates, sandstones and mudstones, some of which are interbedded with, limestones, diatomites, evaporites and tephra deposits (Lamb et al., 1997; May et al., 1999; Blanco, 2008; Blanco and Tomlinson, 2009; Rech et al., 2010). Interpretations drawn from previous research vary, some suggesting tectonics dominate sedimentation patterns, others interpreting climate as the primary driver of sedimentary deposition. Different interpretations also exist as to

* Corresponding author. Tel.: +1 717 291 4388; fax: +1 717 291 4186.

E-mail address: cdewet@fandm.edu (C.B. de Wet).

whether deposition of limestone resulted from an increase or decrease in the water budget of the basin.

The focus of this study is a limestone deposited in the Late Miocene to Early Pliocene, the Opache Formation. We address contrasting views of sedimentation drawn from the Opache Formation limestone. We use an integrated approach of GIS/remote sensing information, detailed petrography, and isotope geochemistry to constrain the depositional and diagenetic characteristics of the Opache Formation, elucidating the role of climate versus tectonic influences (de Wet et al., 2012), and how groundwater and precipitation was of sufficient volume to accumulate limestone in a shallow lake and associated palustrine system for ~3.5 Ma, aridity notwithstanding.

1.1. The Calama Basin

The Calama Basin of northern Chile is one of a series of elongate, terrestrial forearc basins located on the western slope of the Andes. At the latitude of the Calama Basin, and its southern neighbor the Salar de Atacama Basin, the Western Andean Slope is split into two branches. The eastern branch is the Western Cordillera of the Andes, and forms the eastern margin of the Calama Basin, while the western branch (the Cordillera Domeyko or Precordillera Highlands) forms the western margin of the Calama Basin (Hoke, 2006) (Fig. 1). Today, the eastern branch of the western slope rises to the 4000 m above sea level plateau of the Southern Altiplano–northern Puna with its crest punctuated by volcanoes which can exceed 6000 m above sea level in height and it has been volcanically active for at least the last 10 Myr. These volcanoes are part of the western side of the Altiplano–Puna Volcanic Complex that covers a large area at the junction of Chile, Argentina and Bolivia (de Silva, 1989). The western branch (the western margin of the Calama Basin) is topographically more subdued and discontinuous. Its uplift history began in the first half of the Cenozoic. A major geologic feature, the N–S trending Domeyko Fault System, also known as the Western Fault, crosses the Calama Basin at the city of Calama (Fig. 1). This strike-slip fault also experienced appreciable downward displacement to the west between the Mid-Oligocene to Early Miocene, but only meter-scale lateral motion has been measured for displacement from Mid-Miocene through the Pliocene (Tomlinson and Blanco, 1997; Tomlinson et al., 2010). The topographic break in the western branch (Precordillera Highlands) at Calama (termed the “Calama constriction”) allowed basin Miocene-aged sediments to accumulate up to 40 km west of the main Calama Basin in a narrow zone (Fig. 1). Basin narrowing at the Calama constriction was due to two topographic features; a knob of Eocene strata (the Calama Hill) that formed a partial barrier across the narrow part of the Calama Basin just west of the present city of Calama (Tomlinson et al., 2010), and a gap in the Precordillera Highlands where the eastern, N–S orientated Calama Basin is reoriented E–W (Fig. 1). While the Calama Basin is considered to have been a closed basin prior to the Early Pliocene (May et al., 1999; Blanco, 2008), it may have been hydrologically connected via groundwater flow to the Quillagua–Llamara Basin, located on the west side of the Precordillera Highlands in the Central Depression, which contains sediments contemporaneous with those in the Calama Basin (Sáez et al., 1999, 2012). Some time after 3 Myr ago, incision of the Loa River formed a surface water connection between the Calama Basin and the Quillagua–Llamara Basin, with drainage to the west (Jordan et al., 2010).

Uplift of the Western Andean Slope is a Neogene phenomenon. To the north of the Calama Basin, almost 3000 m (2810 m ± 1140 m) of uplift of the Altiplano may have occurred between 26 and ~6 Myr ago, with additional 200–550 m of uplift during the last 6 Myr (Garzione et al., 2008; Jordan et al., 2010). At the latitude of the Calama and Salar de Atacama Basins, uplift on the eastern branch of the Western Andean Slope has been continuous for about the last 17 Myr (Jordan et al., 2010) (Fig. 1). Between 17 and 11 Myr, the southern Altiplano–northern Puna rose about 2800 m (± 2500 m), and in the last 10 Myr, further uplift of up to 2300 m occurred, with much of it occurring within

the last 6 Myr (Jordan et al., 2010). Concurrent with uplift in the last 6 Myr on the eastern branch, a maximum 900 m of uplift could have occurred across the western branch, raising and tilting the Calama–Salar de Atacama area relative to the Central Depression (Houston et al., 2008; Jordan et al., 2010) (Fig. 1). The differences between the uplift histories of different segments of the Andes mean that basins on their flanks record different sedimentation patterns through time as the source and supply of siliciclastic material changed over time. Furthermore, the Calama and Salar de Atacama Basins differ in their sedimentation histories because of different subsidence rates between them, and they were affected by different volcanic eruptions that changed the local topography. Our study's use of detailed GIS-derived cross sections and longitudinal profiles provides new information for the Calama Basin's regional slope and the Opache Formation's thickness variations.

Near present-day precipitation patterns were established ~15 Myr ago on the Western slope of the Andes (Alpers and Brimhall, 1988; Rech et al., 2006). Isotopic analyses of carbonate deposited in the Calama Basin during the Neogene indicated that between 6 and 3 Myr ago, deposited carbonate was enriched in ^{13}C and ^{18}O compared to carbonate that formed before or after this period (Rech et al., 2010). From this observation, Rech et al. (2010) concluded that hyperarid conditions led to evaporative loss of the lighter C and O isotopes, and that the hyperaridity was caused by a rainshadow effect due to rapid uplift of the Andes at 6 Myr ago. However, models have indicated that increasing the height of the Andes after a threshold height has negligible effect on aridity compared to changes in surface seawater temperatures (Garreaud et al., 2010), and that onset of hyperaridity should be placed at 3 Myr ago or even closer to the present (Hartley and Chong, 2002; Reich et al., 2009). Analyses of sediments in the neighboring Quillagua–Llamara Basin also indicate less arid conditions during the time when limestone in the Calama Basin had the highest $\delta^{13}\text{C}$ and $\delta^{18}\text{O}$ (Sáez et al., 2012), and that drier conditions existed before and after this period are characterized by negligible sedimentation.

Present day rainfall amounts are <10 mm/yr in the western part of the Calama Basin, increasing to about 200 mm/year above elevations of 4000 m in the east. Yet in the Neogene there was a well developed freshwater carbonate system in which >80 m of strata accumulated. This system, preserved primarily within the Opache Formation, crops out across 850 km², and ages derived from interbedded volcanic ash beds indicate a depositional age from Late Miocene to Pliocene (May et al., 1999) (Figs. 2, 3).

The Opache Formation lies stratigraphically near the top of a succession of siliciclastic sedimentary rocks (conglomerates, sandstones, mudstones) and pyroclastics of the El Loa Group (Fig. 3), which infills basement topography to depths that locally exceed 2000 m. Siliciclastics in the El Loa Group are interpreted as having formed from ephemeral streams, debris flows, and sheet flow flooding events, associated with mid-alluvial fan to distal fan sandflat/mudflat environments (May et al., 1999, 2005; Blanco, 2008; Blanco and Tomlinson, 2009) (Fig. 2, 3). The carbonate-rich Opache Formation is roughly time equivalent to predominantly siliciclastic alluvial deposits of the Chiquinaputo Formation that is exposed on the eastern flank of the basin (May et al., 2005; Blanco, 2008).

Formations within the El Loa Group are bounded by unconformities and contain ignimbrite deposits. Dates from ignimbrites and volcanic ash beds constrain the Group's age to Early Oligocene to Mid-Pliocene (May et al., 2005; Blanco and Tomlinson, 2009) (Fig. 3). According to May et al. (2005) carbonate sedimentation in the Opache depositional environment commenced between 7.82 and 5.76 Ma and ceased sometime after 3.37 Ma. The carbonates of the Opache Formation represent a significant change in depositional style and lithological character from the units preceding them, suggesting that they formed in a period of relative tectonic quiescence, with an associated reduction in siliciclastic transport. Our study refines Opache depositional environments into lacustrine and palustrine facies, and elucidates the

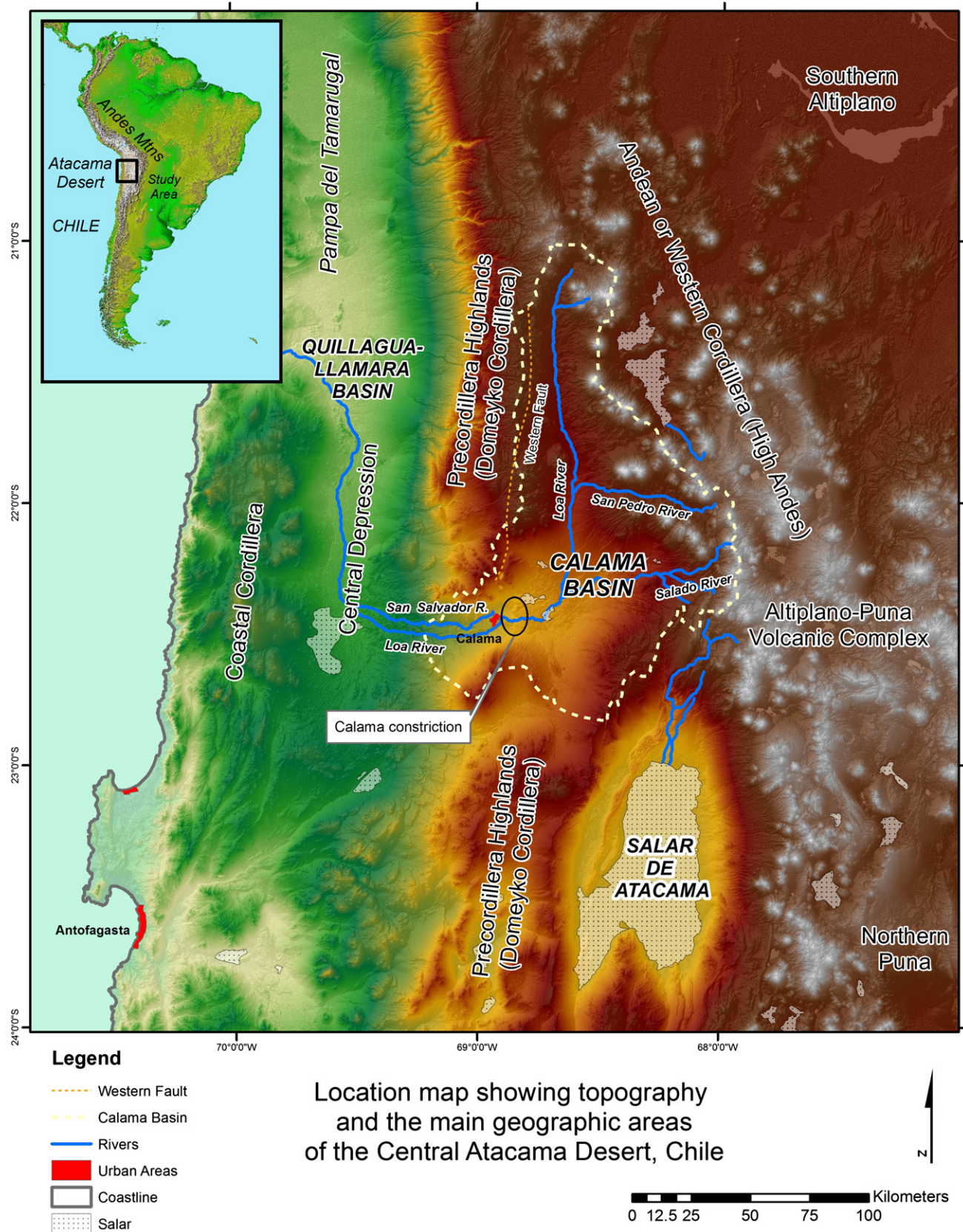


Fig. 1. Location map with GLDEM topography showing the study site in relation to the Pacific Ocean, major topographic and regional features, the Calama Basin and the Calama constriction. The Western Fissure (or Western Fault), also known as the Domeyko Fault System, runs down the axis of the Precordillera Highlands, also referred to as the Cordillera Domeyko.

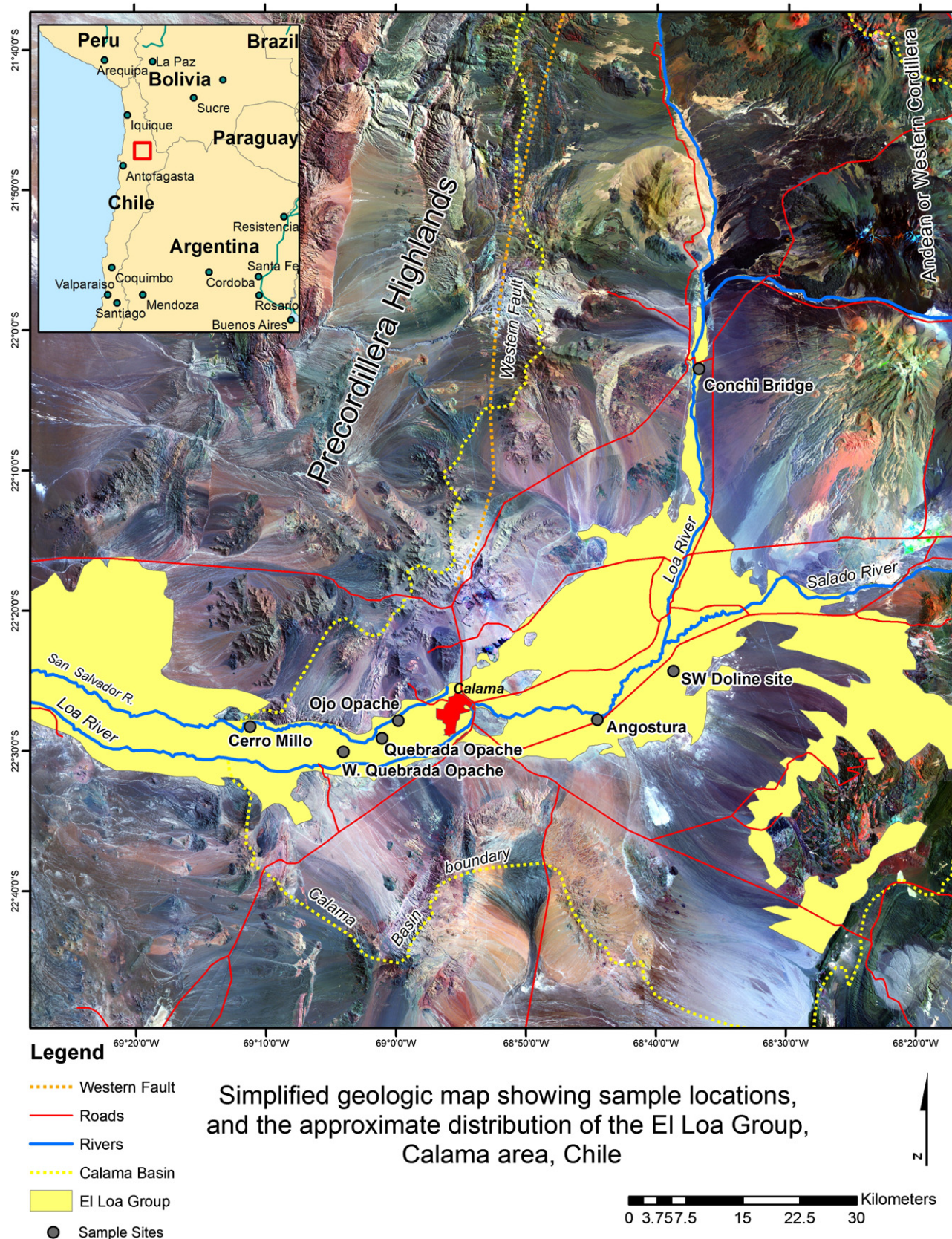


Fig. 2. El Loa Group sedimentary strata distribution, topography and rivers in the study area with Landsat imagery. Sample sites for this study, and the Quebrada Opache site from Rech et al. (2010) are shown. The Cerro Millo location is also referred to as "Col Millo" by May et al. (1999). Our sample location is slightly east of Cerro Millo.

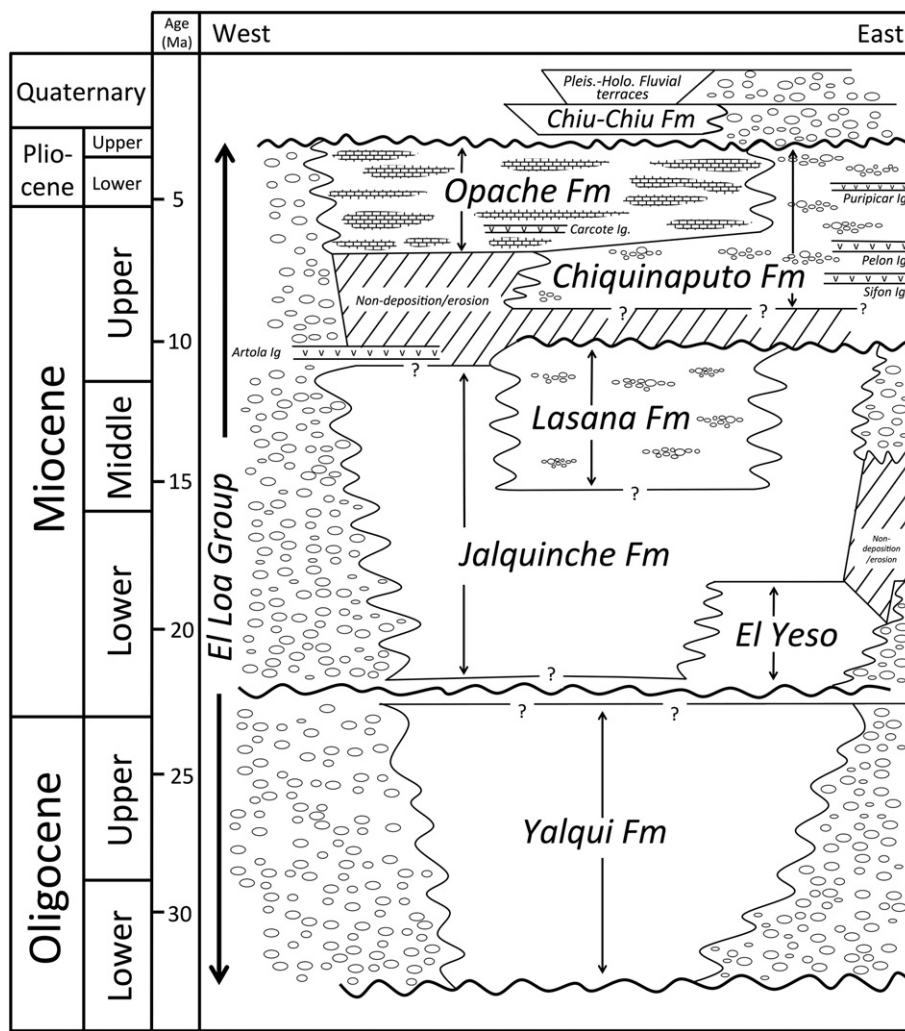


Fig. 3. General stratigraphic relationships within the Calama Basin. Areas without a pattern are sandstone–siltstone lithologies. The Opache Formation consists of predominantly shallow lacustrine and palustrine carbonate strata.

Modified from [Blanco \(2008\)](#) and [Blanco and Tomlinson \(2009\)](#).

role of climate in fostering carbonate production and accumulation during the Late Miocene–Pliocene in the Calama Basin.

2. Methods

2.1. Field

Small alkaline to pH neutral rivers, the Río Loa, Río Salado and Río San Salvador traverse the Calama Basin today in incised canyons where the Opache Formation rocks are well exposed. The canyons formed in the Late Pleistocene when the rivers eroded through the Coastal Cordillera mountains to the Pacific Ocean, resulting in baselevel fall and downcutting ([Sáez et al., 2012](#)). Most of our sampling came from canyon sections, but we also sampled at a doline structure ([Fig. 2](#)). Stratigraphic sections in the canyons were measured and photographed over three field seasons. Representative samples were collected for analyses and site locations documented using global-positioning satellite (GPS) methods.

2.2. Laboratory

2.2.1. Microscopy

Hand samples and 156 thin sections (stained with potassium ferri-cyanide and alizarin red-S, [Dickson, 1966](#)) were described. Scanning

Electron Microscopy (SEM) was conducted at Franklin & Marshall College for detailed study of depositional and diagenetic textures.

2.2.2. X-Ray Diffraction (XRD)

Microsamples of carbonate and non-carbonate fractions (micrite +/- sparry calcite, dolomite and/or silica, evaporate minerals) were obtained using a Dremel microdrill at low rpms. Each sample was microdrilled under a magnifying glass to avoid visibly different constituents. Samples were run at Franklin & Marshall College on a PANalytical X'pet Pro PW3040 X-Ray Diffraction spectrometer using Cu K Alpha radiations, an automated diffraction slit and an X'Celerator detector, according to standard procedures (scans from 6 to 70° 2 theta and a NIST traceable Si metal used to check goniometers accuracy).

2.2.3. Stable isotopes

Chips of limestone were crushed and analyzed for C and O isotopes using a multi-prep device coupled to an Optima dual inlet mass spectrometer at Rutgers University. Samples were reacted at 90 °C for 13 min before transfer to the instrument. Carbon isotopes were also measured in organic matter which was isolated from carbonate by reacting the carbonate overnight in 25% HCl. After removing the acid and washing the remaining organic matter and siliciclastic material, samples were loaded in tin cups and analyzed by CF-IRMS using an Isoprime mass spectrometer coupled to Eurovector elemental analyzer.

Values are reported relative to V-PDB. Strontium isotope ratios were measured from carbonate samples leached with 1 N HCl, as well as from water sampled from the modern Loa, Salado and San Pedro rivers. Strontium was isolated from other elements using standard cation chromatography and analyzed on a GVI Isoprobe at Rutgers University. Long term measurement of SRM 987 has yielded 0.710241 ($\pm 0.000010\sigma$).

2.2.4. GIS methods

Several datasets were combined into an ArcGIS database and used for the analysis of topographic and spatial variations across the study area. Topographic profiles and cross-sections were derived from the 90-meter world digital elevation data from the Shuttle Radar Topography Mission (SRTM). The data was downloaded from the Global Land Cover Facility (GLCF), University of Maryland Department of Geography. Individual tiles were mosaicked together to provide continuous coverage over the study area. The 90-meter spatial resolution and typical vertical resolution of several meters of this data set are sufficient to provide accurate profiles for regional analysis.

The Landsat image is part of the ETM + GeoCover mosaic (S-19-20). The data was collected between 1999-08-20 and 2002-06-27 and was downloaded from GLCF. The image includes three Landsat ETM + bands (7, 4, 2), each sharpened with the panchromatic band and has a spatial resolution of 14.25 m (MDA Federal, 2004).

Road and river data were obtained from the GeoCommunity website (www.geocomm.com) and modified based on aerial and satellite images. Geological contacts were digitized and modified from Blanco (2008), Blanco and Tomlinson (2009), and Rech et al. (2010).

3. Basin configuration

SRTM elevation data shows a broad basin developed east and north of Calama – the Calama Basin (Fig. 1). The majority of the basin is oriented north-south between the Precordillera to the west and the Andes (Western Cordillera) to the east, but extends in a narrow valley east-west for about 40 km through a constriction in the Precordillera Highlands at Calama. The Calama Basin existed as an endorheic basin at least until ~6 Ma ago (May et al., 1999; Blanco, 2008) when lateral movement on the Western Fault created the narrow E-W orientated extension of the Calama Basin (Fig. 1). West of the Calama Basin, the diatomite-rich Quillagua Formation in the Quillagua-Llamara Basin (Fig. 1) formed in shallow, N-S trending lakes (May et al., 1999; Sáez et al., 2012). There is no evidence for a surface water hydrologic connection between the Calama and Quillagua-Llamara Basins until after Opache deposition had ceased and the Ríos Loa and San Salvador incised their channels, connecting the two basins. Longitudinal profiles and topographic cross-sections along the Río Loa show a current regional slope of approximately 0.67° (1.17% grade) between Conchi Bridge (cross-section A-A') and Cerro Milló (cross-section F-F') (Figs. 4, 5, 6). However, the current gradient is higher north of Chiu-Chiu where the slope is 0.71° (1.25% grade) between Conchi Bridge (cross-section A-A') and Chiu-Chiu (cross-section C-C'); and west of Calama where the slope is 1.24° (2.16% grade) between Ojo Apache (cross-section E-E') and Cerro Milló (cross-section F-F') (Figs. 5, 6). The current gradient is much less in the central part of the basin where the slope between Chiu-Chiu (cross-section C-C') and Angostura (cross-section D-D') is 0.09° (0.15% grade); and between Angostura and just east of Calama is 0.50° (0.87% grade) (Figs. 5, 6).

The basin is relatively narrow in the area of Conchi Bridge where the Opache Formation occurs over a width of less than 2 km and broadens in the area of Chiu-Chiu and Angostura (Opache Formation >20 km wide) and then narrows west of Calama between Ojo Apache and Cerro Milló (Apache Formation <10 km wide) (Fig. 5). The current slope would have precluded contemporaneous lacustrine accumulation across most of the basin, except in the area between Chiu-Chiu and Angostura where the modern gradient is very low (Figs. 5, 6). To

generate the accumulation of Opache sediments east of Calama, the current topography suggests that there must have been post-depositional subsidence +/- compaction to produce the present-day relief (Fig. 6). However, as documented by Houston et al. (2008), the Calama Basin experienced significant Miocene–Pliocene deformation, including tilting, fold dome formation, monocline and thrust faulting, and slumping. Interestingly, Houston et al. (2008) note that the Opache Formation in the area between Angostura and Calama is undisturbed and lacks features associated with tectonic activity. This corresponds well with our GIS data indicating that the same area has the lowest gradient, supporting the contention that it remained relatively stable throughout the Miocene–Pliocene period, and post-Pliocene salt pans and wetlands around Angostura indicate that this stability continues today. The current gentle westward gradient west of Calama likely has persisted since at least the Upper Miocene based on the interpretation that the Opache in the area was largely deposited in a palustrine environment rather than in a lake (Fig. 6). Field relations and GIS transects suggest that structurally-controlled topographic relief formed a narrow zone near present-day Calama, we call here “the Calama constriction” (May et al., 2005; Sáez et al., 2012) (Fig. 1).

4. Facies and diagenesis

4.1. Facies associations

May et al. (1999) divided the Calama Basin's Miocene to Pleistocene sedimentary deposits into five facies associations: alluvial fan, fluvial, fluvio-lacustrine diatomite, palustrine carbonate, and massive anhydrite. This study focuses exclusively on the Upper Miocene to Lower Pliocene Opache Formation that constitutes May et al.'s (1999) palustrine carbonate facies association. Within that facies association we recognize two facies: lacustrine and palustrine (Table 1). We document distinct diagenetic characteristics for each facies, but also note a stage of syn-sedimentary diagenesis that contains features indicative of subaerial exposure and pedogenic modification transitional between lacustrine and fully palustrine conditions (Table 1). This intermediate stage represents a depositional hiatus when vadose zone diagenesis affected the lacustrine facies strata for a relatively short period of time and was not repeated, unlike in palustrine settings where subaerial exposure occurs frequently.

Continental carbonates form in subaqueous environments with variable depth and areal extent. They are typically classified as lacustrine if they form subaqueously and remain submerged for all of their deposition whereas palustrine carbonates form in very shallow, partially emergent, environments where pedogenesis repeatedly modifies the sediment syn-depositionally (Freytet and Plaziat, 1982). Palustrine and lacustrine facies are frequently intercalated, particularly along the margins of carbonate-producing lakes (Freytet and Plaziat, 1982).

4.2. Lacustrine facies

Opache Formation lacustrine facies consists of 5–50 cm thick peloidal to structureless lime mudstones and wackestones, distinguishable by subtle color changes (buff, tan, pale gray), changes in porosity (fenestral, nodular, or dense fabrics), and sedimentary structures (soft-sediment deformation, water escape structures, burrows, and ripple marks) and fauna (Table 1). Intraclasts, peloids (Fig. 7a), ostracods (Fig. 7b), diatoms (Fig. 7c), oncoids, gastropods, ooids (rare) and *Charophyte* oogonia are moderately abundant, forming bioclastic wackestones. Dolomite is finely disseminated throughout the lacustrine limestones, but increases upsection, in conjunction with abundant gypsum and less abundant halite (Tables 1, 2). Syndepositional precipitation of gypsum, chert, and non-ferroan dolomite likely contributed to early lithification, as these minerals occur as intraclasts and crusts, as well as replacement

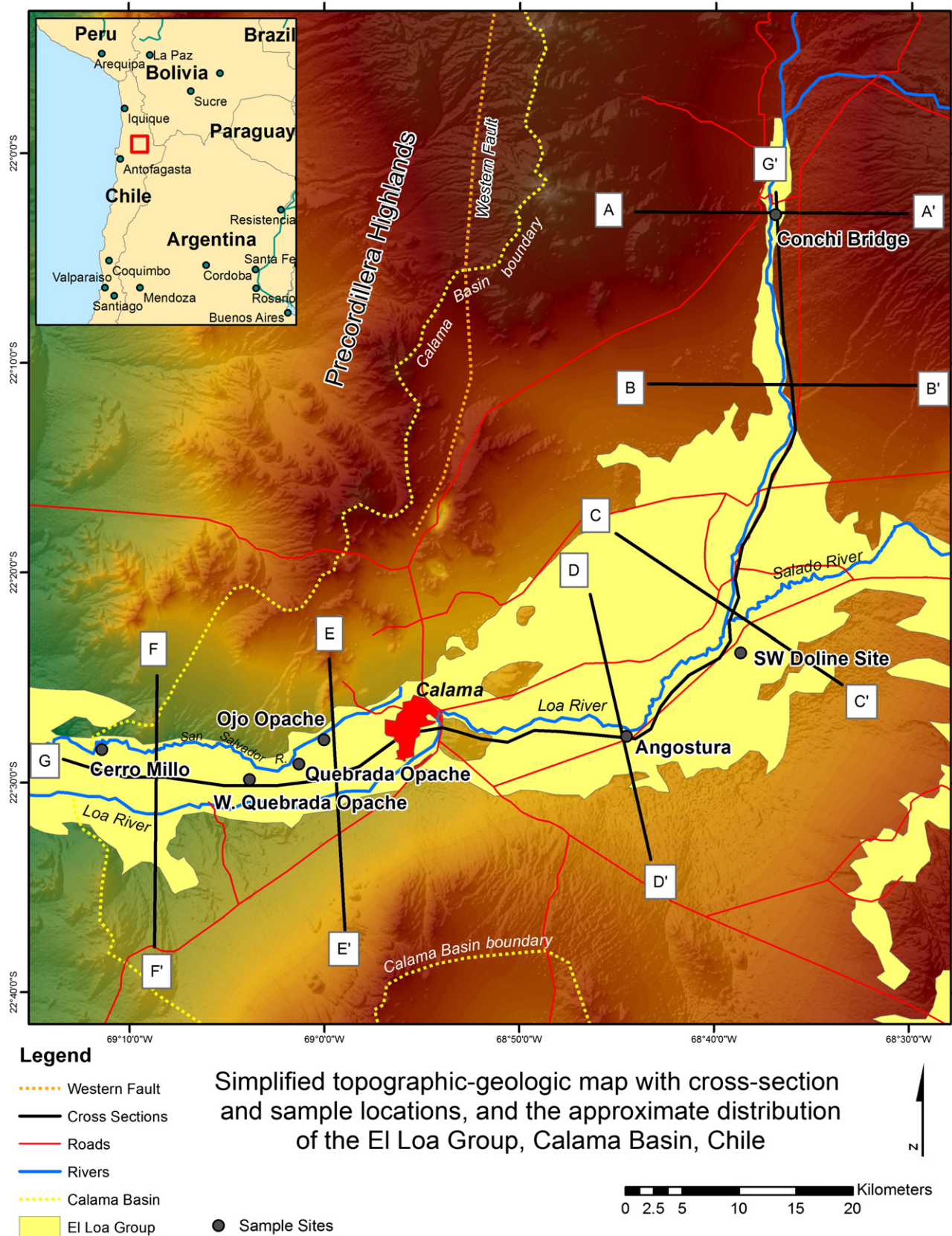


Fig. 4. Cross section locations across the Calama Basin. The cross sections are in Fig. 5.

fabrics and cements. Volcanic glass shards (ash), and siliciclastic sand to silt-sized grains are common constituents in the lacustrine facies (Fig. 8).

Buff-to-gray-colored, well bedded limestone crops out along the canyons and valleys of the Loa and Salado rivers east of Calama (Fig. 1) and constitutes most of the lacustrine limestone facies. This

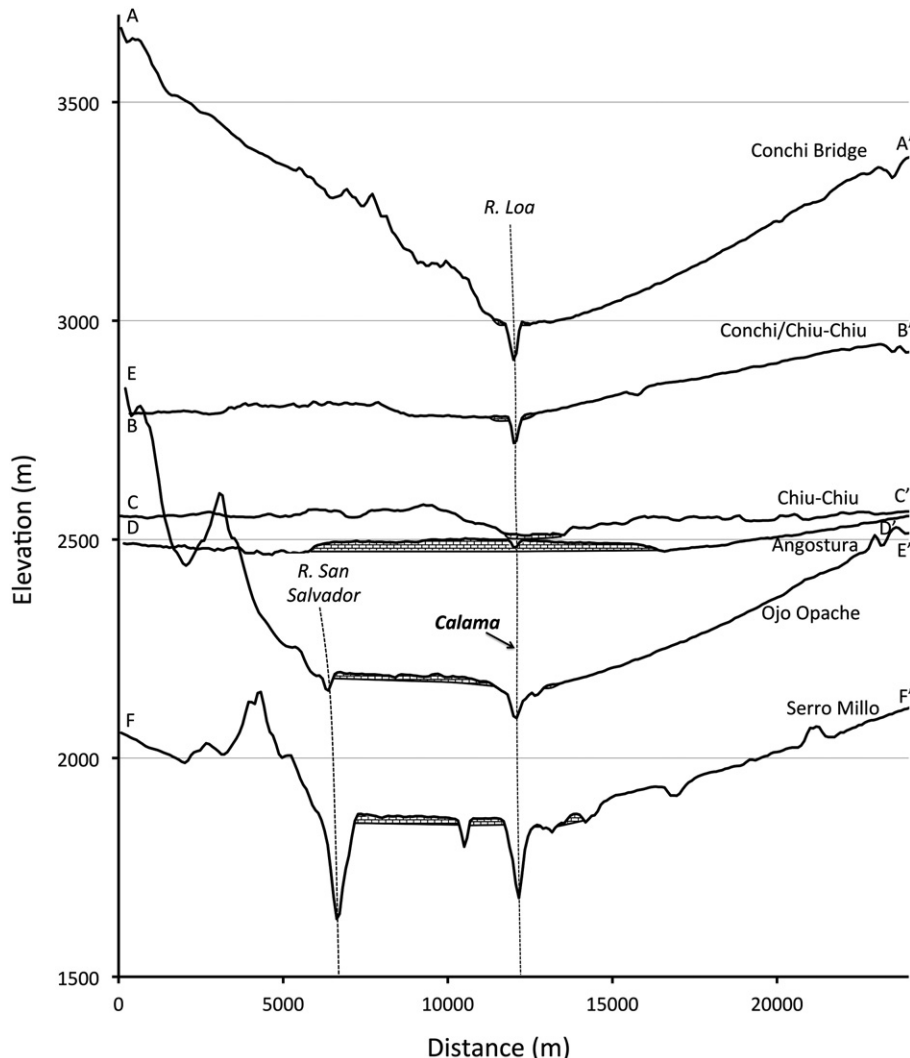


Fig. 5. GIS-derived reconstructions of the topography via local cross sections showing present river canyons and associated gradients. Approximate distribution and thickness of the Opache Formation shown in gray limestone pattern.

facies is well exposed at Angostura (Figs. 2, 9), where a stratigraphic section 41.25 m thick (minimum thickness, since the base is not exposed at this location) is exposed for ~2 km along the canyon (Fig. 10). This study's measured section, closely spaced sampling, and stained thin section petrography is the first detailed published analysis of the Angostura section that we are aware of. Stratigraphically, the lowermost 2 m at Angostura consists of oncoids, peloids, intraclasts, Charophyte oogonia, diatoms, gastropod, and ostracod fossils in clotted and bioturbated micrite. Carbonate allochems form ~90% of the clasts. Unweathered, angular volcanic glass shards (ash) and siliciclastic silt-to-fine sand-sized grains, predominantly quartz, feldspar, biotite and mafic minerals form approximately 10% of the rest of the clastic material, except in mm-to-cm thick horizons where such grains constitute >50% of the sediment. The matrix is calcite, with minor amounts of high-Mg calcite, gypsum, and amorphous silica (Table 2). The lowermost 2 m at Angostura also has secondary features such as stromatactis-like subhorizontal fenestral fractures lined with calcite spar, vuggy porosity, and vadose silts.

Bioclastic wackestone, micrite, and sandy-silty micrite strata constitute the next 35 m of the Angostura section (Figs. 8, 10). Diatoms and ostracods are abundant throughout the beds, with horizons rich in clotted algal or microbial (sensu Freytet and Plet, 1996) textures and oncolites interspersed within them. Eighteen and one-half meters up from the base of the accessible section, a 20 cm thick bed composed of

>80% quartz silt, volcanic glass shards (ash) and biotite, in a green silty matrix, interrupts the carbonate strata. This ash bed forms a distinctive horizon in the field. Bioturbated micrite with ostracod carapaces and diatom tests overlies the ash bed. Similar layers of quartz-biotite-volcanic glass-rich grains in a calcite matrix occur episodically through the remaining stratigraphic succession and siliciclastic grains are scattered throughout the limestone beds in varying proportions.

The ostracod-diatom strata is overlain by sandy-silty limestone that becomes increasingly rich in oncoids, gastropods, ooids (rare) and clotted algal textures upsection, where it grades into a palustrine facies, characterized by platy layers and fenestral porosity (Fig. 11a). Gypsum and halite also increase upsection. Petrographically, root traces, vugs, evaporate minerals and molds, and circumgranular cracks are abundant in the uppermost beds. Angular, silt-to-fine sand-sized siliciclastic grains, volcanic glass shards, and lithic fragments also increase in abundance, forming >50% of the clasts in the top centimeters of the Angostura section. The palustrine facies is described more fully in Section 4.4.

Diagenetic features within the lacustrine facies include first generation isopachous, non-ferroan, equant to dog-tooth calcite spar cement (Fig. 11b) and micrite, typically aggrated to microspar. Second generation non-ferroan calcite spar has both inclusion-rich and inclusion-poor alternating layers within some cavities. Gastropod shells are often

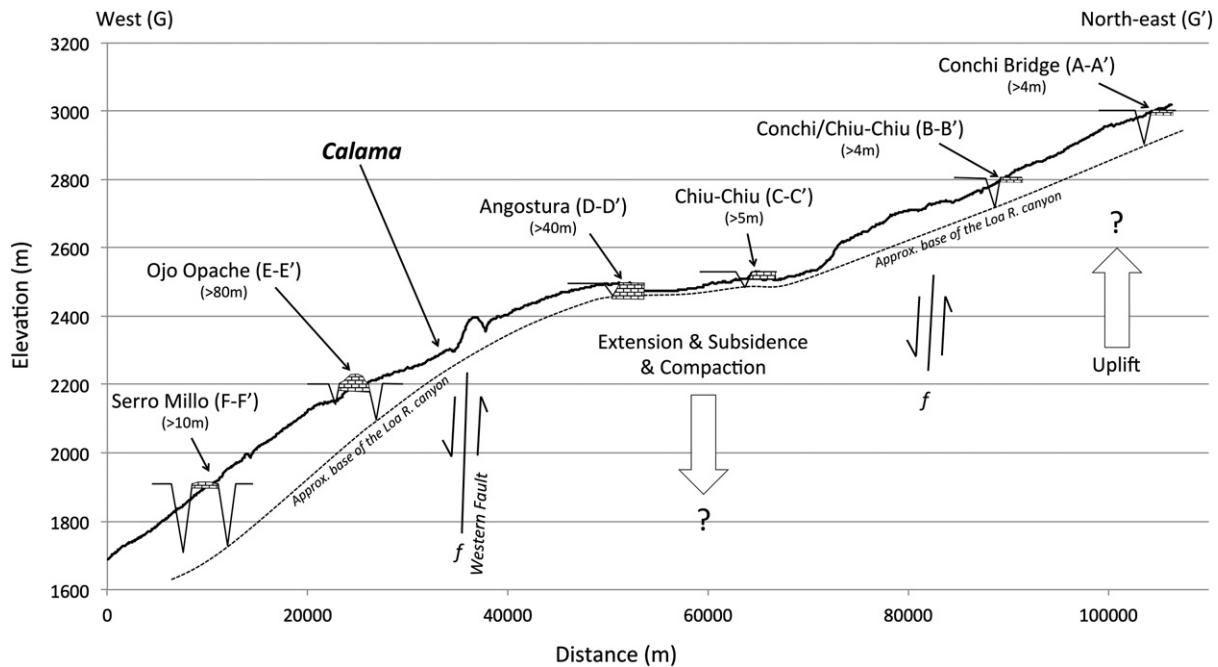


Fig. 6. Longitudinal profile showing present topographical relationships between incised river canyons, approximate Opache Formation thicknesses, and the regional slope. There must have been subsidence and compaction, likely accompanied by local faulting, after Opache deposition, to account for the present relief. Approximate thickness of the Opache Formation shown in gray limestone pattern.

preserved only as molds or casts, indicating dissolution of aragonite (Fig. 11a). Limestone replacement by chert and amorphous silica is common (Fig. 11b) and dolomite, gypsum and halite minerals are present in minor amounts (Table 2). Meniscus and pendant micritic cements occur in the lower 2 m and upper 4.25 m at Angostura.

4.3. Lacustrine facies interpretation

Shallow water indicators such as ripple marks, bioturbated, non-laminated wackestones and mudstones with faunal assemblages of *Charophytes*, ostracods, oncoids, and diatoms, are characteristic of

Table 1
Lacustrine (left side) and palustrine (right side) carbonate facies with depositional and diagenetic features. The middle column lists diagenetic features that are associated with one phase of subaerial exposure and pedogenesis in lacustrine carbonates exposed at Angostura, on the east side of the Calama constriction.

Opache Formation carbonate facies		Syn-sedimentary diagenesis associated with subaerial exposure	Palustrine wackestone, packstone, and grainstone	
Depositional features	Diagenetic features		Depositional features	Diagenetic features
<ul style="list-style-type: none"> – Peloidal to structureless micrite – Ostracods – Diatoms – Oncolites – Gastropods – <i>Charophyte</i> oogonia – Ooids (rare) – Intraclasts – Burrows – Bioturbated fabric – Soft-sediment deformation – Water escape structures – Asymmetric ripple marks – Volcanic glass shards (ash) and siliciclastic sand to silt-sized grains 	<ul style="list-style-type: none"> – Isopachous, non-ferroan low-Mg (less abundant high-Mg) calcite – Micrite, generally aggrated to microspar – Inclusion-rich and inclusion poor second generation equant to bladed calcite (low-Mg) – Dolomite^a – Gypsum^a – Amorphous silica and chert^a – Halite^a 	<ul style="list-style-type: none"> – Fabric-specific moldic porosity; especially gastropod-aragonite, volcanic glass, and evaporate mineral, dissolution – Vadose zone calcite cements: meniscus and pendant – Vuggy porosity – Fenestral pores – Shrinkage and circumgranular cracks – Vertical mudcracks 	<ul style="list-style-type: none"> – Peloidal to fossiliferous micrite to grainstone – Oncolites – Gastropods – Ooids – Stromatolites – Intraclasts – Peloids – Ostracods – Diatoms – Algal mats – <i>Charophyte</i> oogonia – Burrows – Volcanic glass shards (ash) – Plant root traces – Terrigenous siliciclastic cobble to silt-sized grains 	<ul style="list-style-type: none"> – Equant to dog-toothed low-Mg calcite cement in primary and secondary pores – Micrite, aggrated to microspar – Dolomite^a – Gypsum (rare)^a – Amorphous silica^a – Mn-dendrites

^a These precipitates may have formed both syn-depositionally and/or diagenetically.

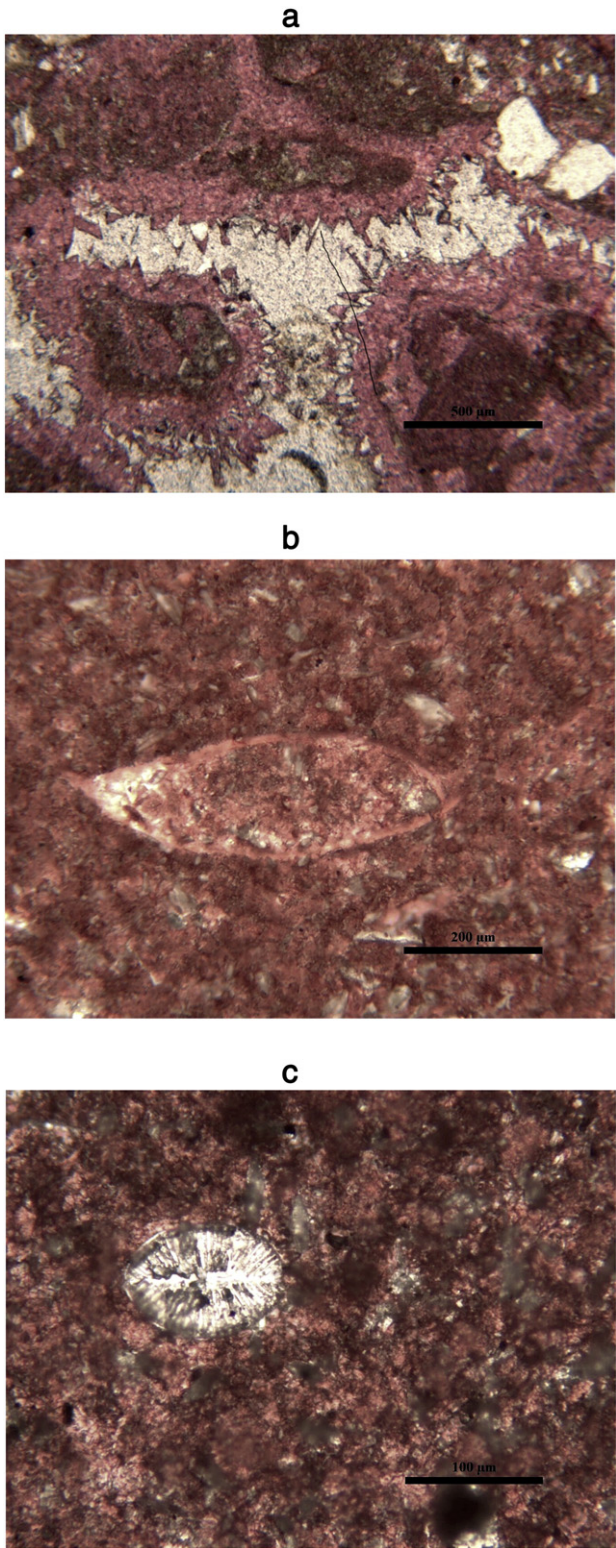


Fig. 7. a. Stained photomicrograph showing intraclasts, peloids and quartz sand grains isopachously rimmed with non-ferroan calcite cement. Yellow is porosity. Conchi Bridge. b. Articulated ostracod with non-ferroan spar, in lacustrine micrite. Gray gypsum crystals and small quartz silt grains are scattered throughout the strata. Angostura. c. Diatom, quartz silt, and gypsum crystals in peloidal bioturbated micrite. Angostura.

shallow lacustrine facies (Peck, 1953, 1957; Birney-de Wet and Hubert, 1989; Pedley et al., 1996; Johnson et al., 2009; Vázquez-Urbez et al., 2012), and typify the Opache lacustrine facies. The diatom-ostracod

faunal assemblage that constitutes most of the Opache Formation's carbonate mudstone–wackestone strata is typical of alkaline lakes today (Dean and Fouch, 1983; Newton, 1994) and indicates similar pH conditions for Opache lacustrine limestone deposition. Clotted and peloidal fabrics characterize the carbonate sediment in many analogous shallow lake systems, such as Plio-Pleistocene deposits in the Guadix Basin, Spain (Pla-Pueyo et al., 2009), demonstrating a microbial presence and active infauna during deposition (Coschell and Rosen, 1994). In the Opache lacustrine facies, similar clotted and peloidal textures suggest that microbial and burrowing faunal communities were present.

Diatom and ostracod mudstone to wackestone lithologies indicate relatively quiet water conditions where micrite was likely generated by bio-induced algal blooms, as occurs in many modern alkaline lakes (Dean and Fouch, 1983; Wetzel, 1983), with additional bioclastic contributions, as evidenced by the *Charophyte*, oncrolite, and gastropod fossils in Opache strata. *Charophytes* are a macroscopic form of green algae, with roots in littoral zone sediments. *Chara* is particularly abundant in freshwater <2 m deep (Peck, 1953, 1957; Burne et al., 1980), and stems are encrusted with calcium carbonate that may disaggregate to micrite when the algae dies (Dean and Fouch, 1983; Platt, 1989). The presence of fauna such as *Charophytes*, gastropods, diatoms and ostracods in a carbonate matrix indicates an alkaline, oxygenated, relatively shallow, freshwater environment (Peck, 1957; Dean and Fouch, 1983; Nickel, 1983; Birney-de Wet and Hubert, 1989; Casanova, 1994; Pedley et al., 1996; de Wet et al., 1998; Andrews et al., 2004; Pentecost et al., 2006; Ashley et al., 2009), and is interpreted as representing similar conditions during Opache Formation's lacustrine facies depositional time, supported by the presence of bioturbated fabrics and burrow structures, indicative of oxygenated bottom sediments and an active infauna. The lack of any dark, organic-rich, finely laminated sediments within the Opache Formation indicates that depositional conditions were never anoxic, implying that the Opache waters were never strongly stratified or deep. Therefore, we interpret the Opache Formation mudstone–wackestone limestone as a fully lacustrine, but relatively shallow water facies.

Discrete siliciclastic-dominated horizons within this facies formed from ashfalls associated with ongoing volcanism in the Andean arc (de Silva et al., 2006), whereas scattered fine-grained clastic grains reflect eolian deposition and subsequent remobilization by bioturbation within the sediment. The texture and composition of the siliciclastic component reflect an immature weathering regime, indicating minor source rock decomposition and limited grain transport (Folk, 1951), as is typical in many semi-arid to arid settings (Pedley et al., 1996; de Wet et al., 1998).

At Angostura, the lowermost 2 m of section consists of lacustrine mudstone and wackestone, overprinted by features indicative of sub-aerial exposure, such as circumgranular cracking, vuggy porosity, and fenestral pores (Freytet and Plaziat, 1982; Wright and Tucker, 1991; Bustillo and Alonso-Zarza, 2007). We interpret this as evidence that the first phase of shallow lake development was interrupted by a drying event that led to subaerial exposure and alteration of lacustrine sediments by pedogenesis. Lacustrine conditions were re-established at Angostura, as evidenced by the ensuing 35 m of diatom-ostracod-rich mudstone and wackestone, and sandy-silty micrite, as discussed above.

The increase in oncrolites, gastropods, ooids and intraclasts in the upper 4.25 m of the Angostura section suggests an increase in water currents (Nickel, 1983), relative to the ostracod-diatom mudstone–wackestone lithology, in association with shallowing conditions, as evidenced by the presence of vuggy and fenestral porosity, root traces, and circumgranular cracks. The abundance of gypsum, halite, and dolomite also increases upsection. We interpret the upper beds at Angostura as having formed in a palustrine setting, associated with lake drying and contraction, as discussed further in Section 4.4.

Diagenetic features within the Opache lacustrine facies include two phases of calcite cement and microspar formation. Cementation of freshwater limestones may be rapid, driven by seasonal supersaturation

Table 2

X-Ray Diffraction results for lacustrine and palustrine facies from the Angostura field site, east of the Calama Gap. Low-Mg calcite is the most abundant mineral, but minor amounts of high-Mg calcite, gypsum, amorphous silica, and halite are present.

Opache Formation X-Ray Diffraction results			
Sample number	Location	Sedimentary characteristics	Mineralogy
ANG-5-8-1	Angostura	Lacustrine micrite	Calcite, minor gypsum
ANG-10-1	Angostura	Lacustrine micrite with ostracods	High-Mg calcite, amorphous silica
ANG-10-11	Angostura	Lacustrine micrite	High-Mg calcite, amorphous silica
ANG-9	Angostura	Lacustrine micrite	Calcite
ANG-17	Angostura	Palustrine micrite with root traces	Calcite, minor gypsum, halite

of porewater carbonate linked to photosynthesis-induced precipitation or biogenic carbonate precipitation associated with microbial or algal activity, for example, encrustations of algal-precipitated low-Mg calcite on bottles found in Green Lake, New York, USA (Dean and Fouch, 1983). Early calcite cements also include the formation of clots, crusts, isopachous spar around grains, and oncrolite syn-depositional lithification (Dean and Fouch, 1983), all of which occur in the Opache lacustrine facies. Zoned calcite cements, such as the inclusion-rich and inclusion-poor spars described here, reflect alternations in the degree of calcite supersaturation or rate of precipitation (Alonso-Zarza et al., 2006). Inclusion-rich crystal zones may indicate local dissolution of aragonite, leaving relict undissolved material in porefluids that is re-incorporated into the next generation of calcite to precipitate.

Wet recrystallization and micrite aggradation (aggrading neomorphism) are responsible for the lithification of carbonate mud, as described by Bathurst (1975) and Pentecost (2005), with or without the addition of externally-derived carbonate. In the Opache Formation lacustrine facies, early dissolution of gastropod aragonite may have served as a source of CaCO_3 ions for micrite lithification, in conjunction with in situ aggrading neomorphism. Lacustrine mudstones and wackestones that were not affected by pedogenesis are well lithified with low porosity.

In freshwater carbonate systems, the Mg-to-Ca ratio in precipitated calcite increases with increasing Mg-to-Ca ratios in the lake water or pore fluids and high-Mg calcite precipitates when the Mg-to-Ca ratio is between 2 and 12, dolomite may form when the ratio is between 7 and 12 (Dean and Fouch, 1983). Evaporative concentration in semi-arid to arid settings may change the Mg-to-Ca ratio in lake and porewater to precipitate high-Mg calcite or dolomite. Dolomite within the Opache

Formation lacustrine facies is attributed to evaporation-induced lake level fluctuations changing the Mg-to-Ca ratio of the water, and/or groundwater fluctuations, driving geochemical gradients both laterally and vertically through the sediments, as described from many other lake successions (Hay et al., 1986; Spötl and Wright, 1992; Armenteros et al., 1995; Cañaveras et al., 1996; Colson and Cojan, 1996; Hurwitz et al., 2000; Del Cura et al., 2001; Hay and Kyser, 2001; Bustillo and Alonso-Zarza, 2007).

The presence of gypsum in the lower and upper Angostura beds shows that evaporative concentration of ponded water occurred during both the initial and waning stages of Opache lacustrine deposition. The presence of halite in the upper strata indicates increased salinity produced when evaporation significantly exceeds freshwater inflow (Rouchy et al., 1993; Arakel and Hongjun, 1994). Volcanic glass is diagenetically reactive and readily dissolves, reprecipitating locally in the Opache limestones as replacive chert and amorphous silica, similar to conditions described by Bustillo and Alonso-Zarza (2007) from the Madrid Basin and Plio-Pleistocene limestones in the Río Grande rift (Mack et al., 2000, 2012). The presence of halite, gypsum, dolomite, and silica in Opache intraclasts indicates that they formed syn-depositionally, associated with very early diagenesis.

4.4. Palustrine facies

The Opache Formation palustrine facies consists of 20–50 cm thick wackestone, packstone and grainstone beds, rich in stromatolites (particularly west of Calama), oncrolites, gastropods, intraclasts, and siliciclastic sands and gravels (Fig. 12a-d) (Table 1). Ooids, ostracods, diatoms, peloids, *Charophyte* oogonia, and algal mat fabrics are common. Vertical desiccation cracks (Fig. 13), root traces, vugs, fenestral pores, fossil molds, and circumgranular cracks are very abundant, and silt to cobble-sized lithic fragments, as well as quartz, feldspar, and mafic mineral grains, occur in cross-bedded lenses and discontinuous horizons throughout the palustrine facies, but are very abundant west of Calama (Fig. 12d). Gastropod shells generally retain their original aragonite mineralogy, although molds are also present. Geopetal structures occur where gastropod shell fragments form shelter pores that are only partially filled with micrite (Fig. 14a). Stromatolite fabrics consist of mm-to-cm-scale brushy fronds and shrubs that form 2–20 cm relief domes or towers (Fig. 12c). Outer rims may be micritized or encrusted with laminated calcite. Stromatolite material may be reworked as intraclasts or as nuclei in coated grains and ooids. Oncoids consist of similar brushy to shrubby fabric, but were not attached to the substrate and have oval to round shapes (Fig. 12b).

Petrographically, the sediments are rich in diatoms, ostracod and *Charophyte* fragments, interbedded with intraclast-ooid-rich and siliciclastic-rich grainstone horizons. Sorting in the carbonate fraction is generally very good, with well sorted, well rounded carbonate grains consisting of ooids, intraclasts, coated shell fragments and peloids admixed with angular to subangular fine sand sized detrital grains such as quartz, mafic minerals, rock fragments, and glass shards. These mixed sands surround the stromatolites and oncrolites and fill internal spaces within algal structures. Intraclasts range in size from sub-millimeter to 2–3 cm diameter. Interestingly, rounded intraclasts composed of fine-grained dolomite are relatively abundant.

Calcite cements are non-ferroan equant to dogtoothed spar, interspersed with clumped, peloidal micrite locally. Meniscus and pendant cements are common. Dolomite occurs as irregular lenses or patches, or forms intraclasts. Horizons may be well cemented with equant spar, or have significant primary porosity in shelter cavities, intergranular pores, and within algal structures. First generation calcite spar frequently lines internal pores but the crystal tips commonly have jagged and irregular surfaces (Fig. 14b). Manganese oxides, probably pyrolusite +/– iron, occur as dendrites, generally closely associated with cracks or pores (Fig. 14b).

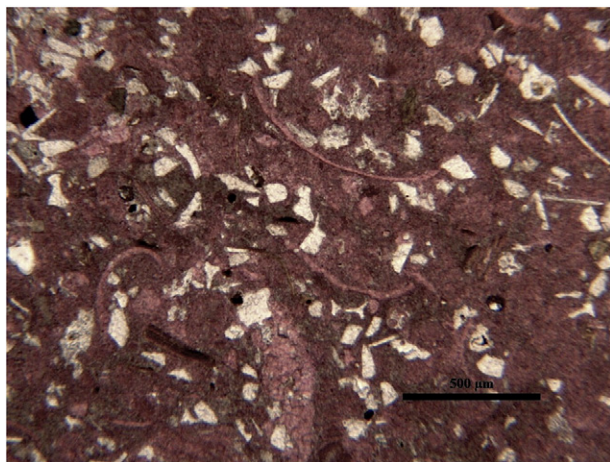


Fig. 8. Photomicrograph of typical Angostura lake strata composed of ostracod-rich bioturbated micrite with ash fall deposits consisting of volcanic glass shards and angular quartz silts. Angostura.



Fig. 9. Field site at Angostura. The Loa River flows in the base of the canyon, having incised through the Opache Formation post-Pliocene. Well bedded limestones are interpreted as having formed in a shallow lake. Basal layers reflect initial lacustrine conditions, interrupted by subaerial exposure and vadose zone diagenesis, followed by deposition of fine-grained, ostracod-diatom-rich micrite, indicating a return to lacustrine conditions, followed by palustrine features in the upper beds as lake sedimentation ceased. Note people in the lower left for scale. See Fig. 10 for our stratigraphic column for this site.

The palustrine facies is well represented by Opache Formation limestone strata exposed west of the Calama constriction. May et al. (1999) defined the type section for the Opache Formation at Quebrada Opache where a section 84 m thick consists of carbonate cemented siliciclastic sands and gravels, overlain by carbonate beds with abundant oncoids, gastropods, ooids, and intraclasts (May et al., 1999, 2005). The authors describe microkarst features, peloids, pisoliths, root traces, gastropods, ostracods, *Charophytes*, and algal laminations (May, 1997; May et al., 1999; Rech et al., 2010). Palustrine facies limestone is also present in the uppermost strata east of Calama; in the top 4.25 m of exposure at Angostura and Conchi, and along the top of Loa River canyon south of Conchi (Fig. 15).

4.5. Palustrine facies interpretation

According to Freytet and Plaziat (1982), palustrine settings are characterized by both subaqueous conditions and subaerial exposure on a regular basis; palustrine fabrics result from exposure and pedogenesis of lacustrine sediments (Freytet and Verrecchia, 2002). In the Opache Formation carbonate strata, beds that contain evidence for very shallow lacustrine deposition, but also contain features indicative of exposure and pedogenesis, are interpreted as palustrine. Evidence for subaqueous deposition includes textures and biota common to the Opache lacustrine facies described previously (Section 4.2), such as ostracod and diatom fossils, *Charophyte* oogonia, intraclasts, peloids and lesser amounts of gastropods and oncolites.

Superimposed on the Opache lacustrine sediments are features demonstrative of syn-depositional alteration. For example, root traces within the Opache limestones indicate the former presence of vegetation, and are commonly associated with palustrine settings (Freytet and Plaziat, 1982; Liutkus and Ashley, 2003). Tannins released by palustrine plants may maintain manganese in a divalent state by lowering the pH of the microenvironment around them, and aquatic macrophytes in general contain much more intracellular manganese than do non-aquatic plants (Mount and Cohen, 1984). This helps explain the common association of pyrolusite +/– other Mn complexes with palustrine carbonates, seen as Mn-oxides halos around rhizoliths, and as dendrites associated with root traces and early shrinkage or

desiccation cracks, like those observed in the Opache palustrine limestones (Mount and Cohen, 1984; Ashley et al., 2014).

Vertical desiccation cracks, circumgranular cracks, and, aragonite dissolution and vuggy porosity reflect vadose zone processes where drying, sediment shrinkage, and fluids undersaturated with respect to calcium carbonate move through the sediment, as documented from continental limestones similar to Opache palustrine facies (see Freytet and Plaziat, 1982; Bustillo and Alonso-Zarza, 2007). Alternations of wet and dry conditions contribute to intraclast formation via in situ brecciation during desiccation followed by reworking during reflooding periods (Freytet and Plaziat, 1982; Esteban and Klappa, 1983; Alonso-Zarza et al., 2012). Intraclasts are a very common constituent of the Opache palustrine facies, and are interpreted as evidence that the palustrine sediments experienced subaqueous to subaerial conditions multiple times. Rounded dolomite intraclasts have not been previously reported from the Opache limestones, but indicate that at least some of the dolomite in the succession must be syn-depositional so that it could be eroded and reworked intrabasinally. Similarly, silica and gypsum occur within palustrine facies intraclasts, also indicating their early origin. Palustrine evaporation and flooding events rapidly change porewater saturation states such that volcanic glass (ash) readily dissolves, but may reprecipitate locally as amorphous silica, and calcite and gypsum may precipitate during times of supersaturation, as documented from palustrine successions elsewhere (Freytet and Plaziat, 1982; Alonso-Zarza et al., 2006; Valero Garcés et al., 2008).

Opache palustrine limestones, particularly those exposed west of the Calama constriction, also contain evidence for flowing water. For example, the presence of oncolites, ooids, well sorted carbonate sands, and lenses of crossbedded gravel to sand sized siliciclastic material, all indicate current activity. Because stromatolites are well developed and abundant in the Opache strata west of the Calama constriction, where they occur in close association with the features listed above, they likely thrived in gently moving water. Freshwater stromatolites occur in numerous Pleistocene–Holocene settings, for example, in the Cuatro Cienegas basin, Coahuila, Mexico (Golubic, 1991), Green Lake, New York, USA (Dean and Fouch, 1983) and Lake Bogoria, Kenya (Casanova, 1986), having in common alkaline waters with stromatolites growing in a non-stagnant photic zone. Stromatolites form from a

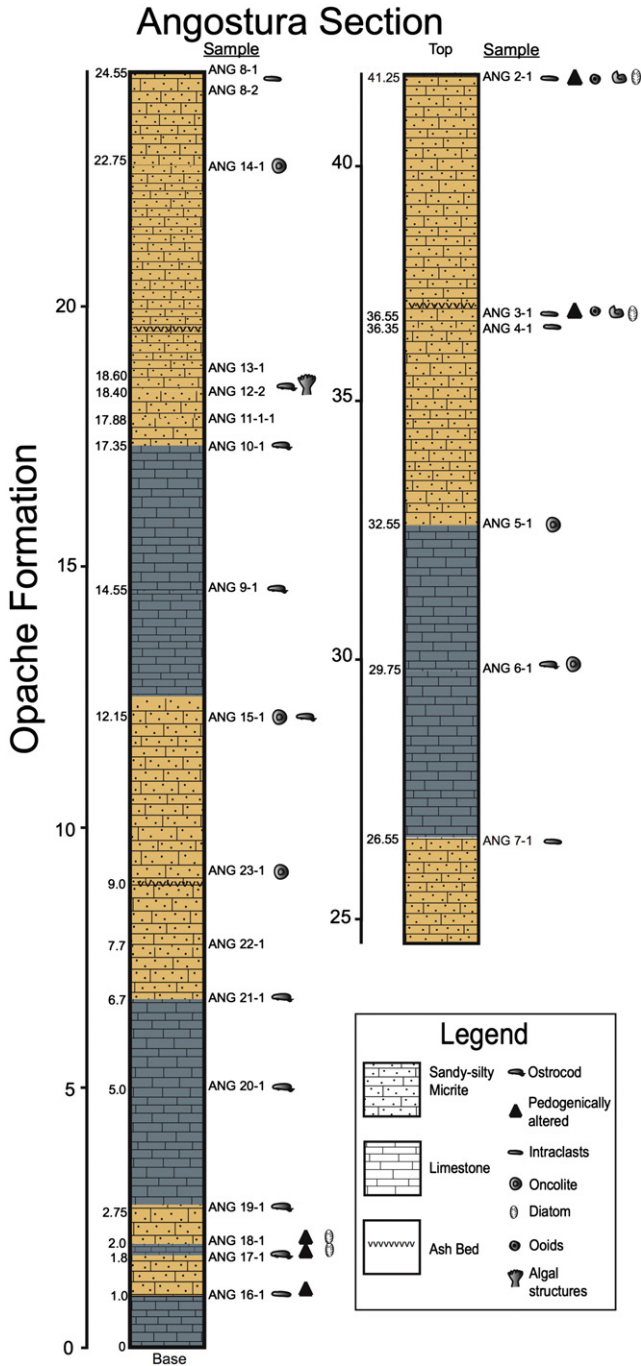


Fig. 10. Measured section from the Angostura site. The section starts in the bottom of the canyon at river level, this may not be the base of the Opache as the Opache Formation-Chiquinaputo Formation contact is not exposed. The lower 2.5 m and upper 5.25 m contain evidence for subaerial exposure and pedogenesis, however, most of the Opache Formation at Angostura is interpreted as a lacustrine facies. Lithologic boundaries between the sandy-silty micrite and limestone as drawn on the stratigraphic log are approximate.

range of calcifying cyanobacteria (+/− bacterial) communities and host diverse populations of molluscs and fish (Monty and Hardie, 1972; Golubic, 1991; Chafetz and Guidry, 2003). Petrographically, brushy fronds and peloidal clots within the Opache stromatolites bear similarities to shrubby, thrombolitic microbial stromatolites and oncolites described from East African rift lakes (Casanova, 1994).

Oncolites, or mobile, nodular structures composed of laminated algae and/or cyanobacteria around a nucleus, indicate moderate water current activity, of sufficient velocity to overturn the oncrites episodically (Nickel, 1983; Golubic, 1991). The abundance of oncrites in the

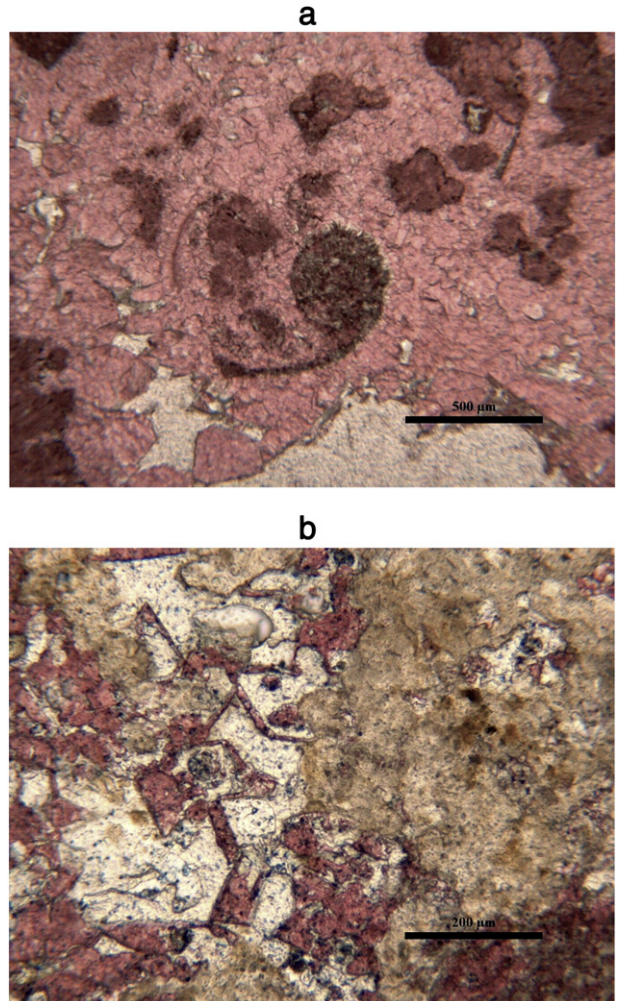


Fig. 11. a. Partially dissolved gastropod shell associated with vuggy porosity, subsequently occluded with non-ferroan equant to dog tooth sparry cement. Gypsum crystals, seen here as small gray fringe-like crystals, selectively precipitated in the gastropod's micritic infill. Angostura. b. Dog tooth calcite spar and primary micrite matrix partially replaced with chert and amorphous silica (pale brown color). White color is porosity. Conchi Bridge.

Opache palustrine strata indicates deposition with moderate current activity. Taken together, evidence indicates that the palustrine sediments deposited west of the Calama constriction experienced greater current activity than did the lacustrine carbonates that formed east of the Calama constriction, indicating shallower water and exposure to higher energy events, supporting our interpretation of a palustrine depositional environment.

We interpret cross bedded grainstone and siliciclastic sands and gravels within the palustrine facies as having formed from episodic flood or high energy events, capable of eroding channels through shallow-water paludal sediments. The region's Late Miocene–Pliocene aridity meant that carbonate production usually dominated Opache sedimentation, and that a lack of surface water minimized weathering and erosion of siliciclastic debris, however, the presence of poorly sorted (cobble to sand-sized), cross-bedded, clastic material in localized, discontinuous channels and scours, such as we observe in the palustrine strata west of the Calama constriction, indicates that flashy, episodic, high energy storm events transported siliciclastic material into the palustrine environment. Cobble-sized clasts were transported a kilometer or more from the Precordillera Highland source area into the palustrine setting west of Calama where the largest cobbles occur.

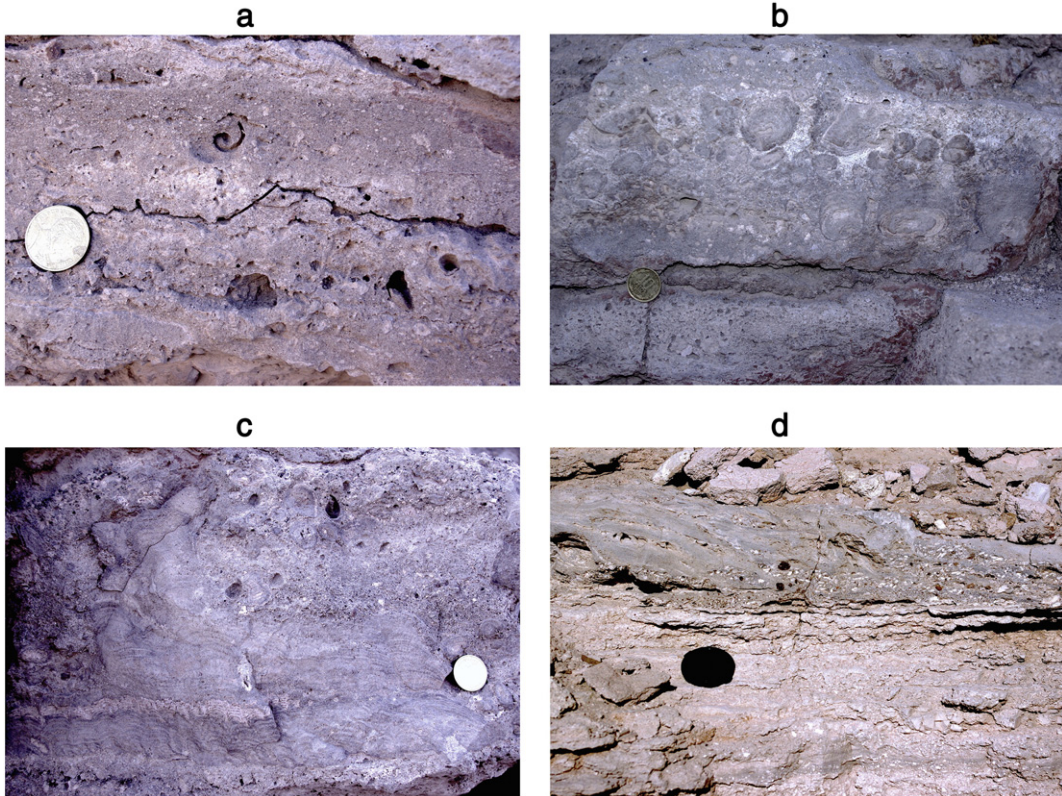


Fig. 12. Palustrine limestones from field locations west of the Calama constriction. 2 cm diameter coin for scale. a. Gastropod molds and preserved gastropods are abundant, as well as intraclasts (white clasts in this photograph). West Quebrada Opache Site. b. Oncolites in an intraclast-laden (white clasts) micrite matrix. West Quebrada Opache site. c. Stromatolitic limestone overlain by intraclast-rich packstone/grainstone with gastropod molds. East of Cerro Millo site. d. Palustrine limestone (lower third of the photo) with abundant intraclasts (white clasts), overlain by cross bedded sands and gravels containing fresh (unweathered) lithic fragments, intraclasts, and quartz grains. Lens cap is 5.5 cm diameter. East of Cerro Millo.

Diagenetic reactions in palustrine settings are closely linked to pedogenesis and may occur multiple times while sediment is accumulating, depending on the frequency and duration of subaerial exposure. Water table fluctuations between vadose and phreatic conditions typically yield aragonite dissolution and reprecipitation of carbonate as cements, vadose silts, crusts and intraclasts, such as those documented in the Opache palustrine facies (Fig. 12d). Freytet and Plaziat (1982) and Alonso-Zarza et al. (2006) interpret similar textures and features as having formed through water table fluctuations in palustrine environments. Meniscus and pendant cements, described from marine and continental limestones, indicate that sediments experienced cementation within the vadose zone where both air and water occur in the

pores (Bathurst, 1975; Platt, 1989). These cement phases within the Opache palustrine facies limestones indicate subaerial exposure and calcite cement precipitation under meteoric vadose conditions. Opache palustrine limestones also exhibit one generation of diagenetic non- to weakly ferroan, equant to dogtooth calcite inter- and intragranular spar. Since the spar isopachously lines cavities and evenly rims grains it is interpreted as having precipitated under phreatic conditions, where the pores were filled with meteoric water supersaturated with respect to calcite (Bathurst, 1975; Purvis and Wright, 1991). Jagged, partially dissolved calcite crystal faces inside some cavities indicate that undersaturated fluids migrated through the Opache limestone after initial cement precipitation, interpreted as further evidence of multiple exposures to vadose zone undersaturated porefluids. Only partially occluded primary porosity, however, suggests that diagenetic cement precipitation became negligible when Opache Formation sedimentation ceased.

5. Stable isotopes

5.1. Oxygen and carbon

Oxygen and carbon isotopes were measured in bulk carbonate through the section at Angostura (Table 3). Selected samples were also microdrilled to assess potential isotopic variation between primary carbonate and diagenetic carbonate (Table 4). Peloids, oncrites, ooids, and blocky cements were microsampled. In bulk samples, $\delta^{18}\text{O}$ varies between $-5.50\text{\textperthousand}$ and $-3.26\text{\textperthousand}$, averaging $-4.24\text{\textperthousand}$, and for $\delta^{13}\text{C}$, between $+2.46\text{\textperthousand}$ and $+4.35\text{\textperthousand}$, averaging $+3.27\text{\textperthousand}$ (Tables 3, 4). Similarly to the Ojo Opache section described in Rech et al. (2010), a correlation exists between $\delta^{13}\text{C}$ and $\delta^{18}\text{O}$, but its r^2 value is only 0.26 compared to 0.43. The combined datasets produce a correlation of 0.73. These correlations indicate that, to a large extent, evaporation is



Fig. 13. Mudcracked palustrine sediments. East of Cerro Millo.

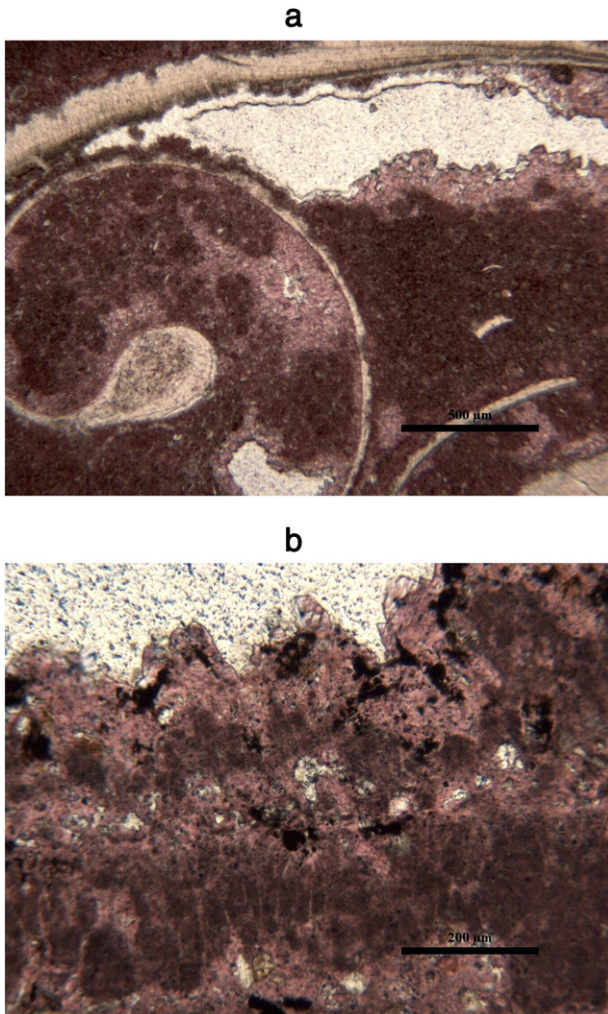


Fig. 14. Depositional and diagenetic features from palustrine Opache strata west of the Calama constriction. a. Aragonitic skeletal gastropod forming a shelter pore, partially filled with micrite and non-ferroan sparry calcite. Small pendant micrite cements hang from the cavity ceiling. White space is open porosity. Pelleted micrite fills much of the gastropod chamber. W Quebrada Opache. b. An open vug (white), lined with partially corroded non-ferroan calcite, overlying peloidal micrite with pyrolusite dendrites (black features). East of Cerro Millo.

Table 3

Stable isotope compositions of organic carbon, and calcite carbon and oxygen for samples collected at Angostura, on the east side of the Calama constriction. All samples are reported relative to the V-PDB standard.

Sample	Height (m)	$\delta^{13}\text{C}_{\text{org}}$	$\delta^{13}\text{C}_{\text{carb}}$	$\delta^{18}\text{O}_{\text{carb}}$
ANG2	41.25	-24.93	2.46	-4.11
ANG3	36.55	-26.87	2.47	-4.70
ANG4	36.35	-27.11	2.24	-4.68
ANG5	32.55	-15.24	3.35	-3.50
ANG6	29.75	-29.75	4.43	-4.39
ANG6	29.75	-29.75	4.86	-4.35
ANG7	26.55	-25.12	3.77	-3.94
ANG8.1	24.55	-28.38	3.51	-3.84
ANG8.2	24.55	-28.21	3.35	-4.09
ANG14	22.75	-22.32	4.04	-3.26
ANG12.1A	18.40	-21.89	3.08	-3.63
ANG12.1B	18.40	-24.8	3.15	-3.64
ANG12.2	18.40	-23.18	3.35	-4.05
ANG11	17.88	-18.13	3.67	-3.30
ANG10.1	17.35	-20.54	3.28	-3.55
ANG10.2	17.35	-19.19	3.04	-3.83
ANG9.1	14.55	-11.25	3.79	-3.52
ANG9.2	14.55	-17.29	3.05	-4.08
ANG15	12.15	-28.68	3.31	-4.59
ANG23	9.00	-27.29	3.06	-4.47
ANG22	7.70	-24.52	2.98	-5.33
ANG21	6.70	-22.07	3.52	-4.62
ANG20	5.00	-12.74	3.82	-4.38
ANG19	2.75	-21.25	3.32	-4.81
ANG18	2.00	-20.92	3.01	-4.52
ANG17	1.80	-24.14	2.89	-4.91
ANG16	1.00	-19.91	2.84	-5.5

responsible for the variation in C and O isotopes, but the weaker correlation exhibited at Angostura suggests that other factors may operate which can alter $\delta^{13}\text{C}$ and $\delta^{18}\text{O}$, or the volume of water in the lake buffered the effects of evaporation on isotope compositions. The pattern of vertical variations in $\delta^{13}\text{C}$ and $\delta^{18}\text{O}$ through the Angostura section is similar to that of the Ojo Apache section (Rech et al., 2010) (Fig. 16), the most depleted $\delta^{13}\text{C}$ and $\delta^{18}\text{O}$ values occur at the base and at the top of the section, but depleted values were measured in limestone 7.7–9.0 m above the base at the Angostura section, and 15–23 m above the base at Ojo Apache. Where primary carbonate and diagenetic cements were sampled individually, their isotopic compositions were generally within 1‰ of each other and overlapped with the bulk sample values (Table 3). However, in the lower part of the Angostura section, the calcite cement C and O isotope compositions are higher than the



Fig. 15. Palustrine facies. Platy weathering limestone with horizons of vuggy to fenestral porosity, located at the top of the Opache Formation east of the Calama constriction. Conchi Bridge.

Table 4

Stable isotope compositions of calcite carbon and oxygen microdrilled from selected samples collected at Angostura. All samples are reported relative to the V-PDB standard.

Sample	Description	$\delta^{13}\text{C}_{\text{carb}}$	$\delta^{18}\text{O}_{\text{carb}}$
ANG2.Am	Ooid	2.36	-3.90
ANG2.Bm	Carbonate clast	2.76	-4.84
ANG2.Cm	Calcite cement	2.65	-4.15
ANG2.Dm	Carbonate clast	2.93	-4.37
ANG2	Bulk	2.46	-4.1
ANG12.1B1m	Dark, crack filling calcite	3.75	-3.88
ANG12.1B2m	Micritic peloid	3.18	-3.11
ANG12.1B3m	White calcite cement	2.65	-3.60
ANG12.1B	Bulk	3.15	-3.64
ANG16.1 m	Void filling calcite spar	3.35	-4.50
ANG16.2 m	Micritic peloid	2.73	-5.00
ANG16.3 m	Micritic peloid	2.50	-5.08
ANG16	Bulk	2.84	-5.5
ANG19.1 m	Micritic peloid	2.68	-4.89
ANG19.2 m	Calcite cement	3.66	-4.50
ANG19	Bulk	3.32	-4.81
ANG21.1 m	Void filling calcite	3.88	-3.70
ANG21.2 m	Void filling calcite	4.17	-4.39
ANG21	Bulk	3.52	-4.62

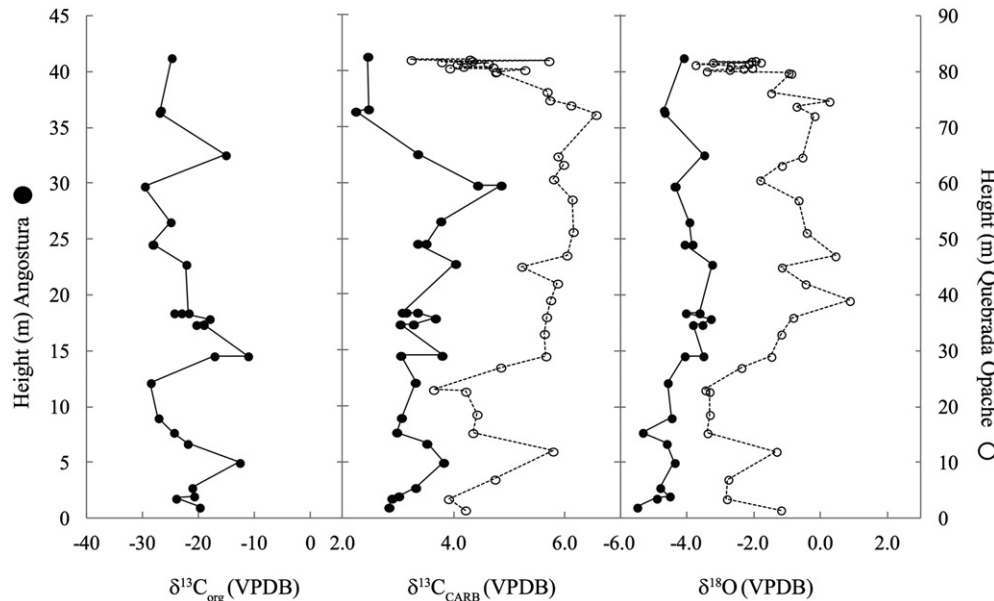


Fig. 16. Organic carbon isotope data from Angostura, and carbonate carbon and oxygen isotopic values from upsection from both Angostura and Quebrada Opache (Quebrada Opache values from Rech et al., 2010).

primary calcite, suggesting that the cement may have been derived from more evaporated water from which CO_2 had escaped. Higher in the section there is no consistent isotopic difference between the cements and primary allochems. The uppermost Angostura beds have a complex mosaic of diagenetic features and yield a mixed isotope signature, relative to the fully lacustrine beds below, indicating that the upper beds were exposed to highly evaporative fluids as well as fresher ones. The fully lacustrine beds were less prone to infiltration by isotopically evolved fluids.

Carbon isotopes measured on organic matter deposited with the Angostura limestones range between $-30\text{\textperthousand}$ and $-10\text{\textperthousand}$, with an average of $-22.4\text{\textperthousand}$ (Tables 3, 4 and Figs. 16, 17). The most negative values occur near the base of the section, around 12 m, and in the uppermost 22 m.

5.2. Strontium

There is small but significant range in Sr isotope composition of the Opache carbonates which falls within the limits of the modern river

system (Table 5). The Río Loa $^{87}\text{Sr}/^{86}\text{Sr}$ composition is 0.70606, the Río Salado, 0.70763, and Río San Pedro, 0.70786. Samples from the Opache from four different locations in the Calama Basin were analyzed: three lacustrine samples from Angostura, bedded carbonate close to the bridge at Conchi, at a fossiliferous palustrine location west of Calama close to Quebrada Opache and a 7 million year old spring deposit in the Chiquinaputo Formation close to the Río Salado. The Chiquinaputo spring has a composition (0.70760–0.70786) that is the same the Salado and San Pedro rivers, indicating that the sources of Sr from the arc have been similar for the past 7 Ma. Apart from the final drying stage of the lake system at Angostura, lacustrine carbonates at Angostura and Conchi have similar $^{87}\text{Sr}/^{86}\text{Sr}$, although carbonate at Conchi is slightly less radiogenic (0.70720) than at Angostura (0.70724 and 0.70734). The palustrine carbonate, sampled a few meters from the top of the Opache west of Calama, has the least radiogenic Sr (0.70641).

6. Discussion

6.1. Continental carbonate accumulation

Continental carbonates are highly sensitive recorders of the interplay between tectonics and climate (Cecil, 1990; de Wet et al., 1998; Alonso-Zarza, 2003; Gierlowski-Kordesch and Buchheim, 2003; Bohacs et al., 2007; Valero Garcés et al., 2008; Bird, 2009; Valdeolmillos-Rodríguez et al., 2011). For terrigenous limestones to form in appreciable quantity there must be relative tectonic quiescence so that they will not be swamped by siliciclastic material. Similarly,

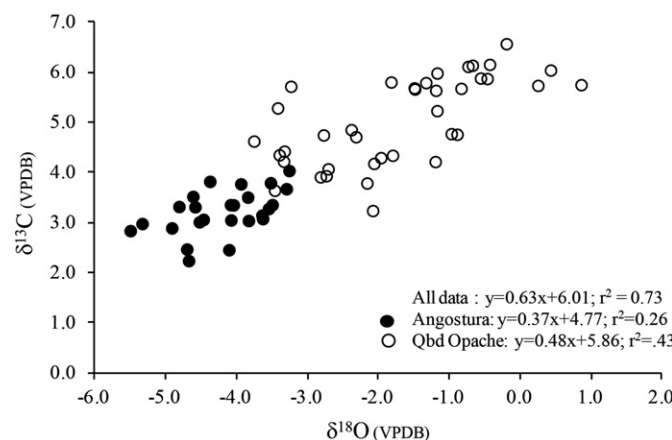


Fig. 17. Stable isotope cross plot comparing data from Angostura (lacustrine facies east of the Calama constriction) with values from Quebrada Opache (palustrine facies west of the Calama constriction) (Quebrada Opache data from Rech et al., 2010).

Table 5
 $^{87}\text{Sr}/^{86}\text{Sr}$ normalized to $^{86}\text{Sr}/^{88}\text{Sr} = 0.1194$, and corrected to NSB 987 = 0.710245 to account for data acquired from different instruments.

Sample	Description	$^{87}\text{Sr}/^{86}\text{Sr}$
Rio Loa	Conchi Reservoir	0.706060
Rio Salado	5 km east Chiu-Chiu	0.707630
Rio San Pedro	DGA gauging station	0.707833
Angostura; ANG 2.1	Opache Fm.	0.706863
Angostura; ANG 10.1	Opache Fm.	0.707340
Angostura; ANG 16.1	Opache Fm.	0.707240
Conchi Bridge site	Opache Fm.	0.707200
Fossiliferous limestone	Opache, near Ojo Opache	0.706410

continental carbonate systems are most productive when rainfall is insufficient to weather and transport large quantities of siliciclastic debris into the carbonate-producing environment, but there must be sufficient water to create conditions necessary for limestone development, such as a lacustrine or palustrine setting. The record of continental carbonates, therefore, indicates that these conditions were met, i.e. that there was relative tectonic quiescence, at least locally, and that the climate was neither too humid nor too arid for limestone production and accumulation (Ashley et al., 2014).

Cecil's (1990) study highlighted the climate versus tectonics controversy and since then much work has been done to tease apart these parameters (de Wet et al., 1998; Gierlowski-Kordesch, 1998; Freytet and Verrecchia, 2002; Alonso-Zarza, 2003; Gierlowski-Kordesch and Buchheim, 2003; Bohacs et al., 2007; Valero Garcés et al., 2008; Johnson et al., 2009; Pla-Pueyo et al., 2009; Valdeolmillos-Rodríguez et al., 2011; Cabaleri and Benavente, 2013). The study of Holocene continental carbonate producing environments has made significant contributions towards unraveling the nuances of climate (*Charophytes* as sensitive, non-equilibrium climate indicators, Andrews et al., 2004) and tectonic influences (e.g. narrow barrage tufas and perched springs as indicators of high relief, Vázquez-Urbez et al., 2012). We can now say with greater certainty that in most cases, low lying continental lacustrine and palustrine systems, such as the Opache Formation, that contain clear evidence for water accumulation and subaerial exposure, with the appropriate suite of fossils and possibly evaporate minerals, are the result of minimal tectonic activity and an arid to semi-arid climate. Such climate conditions have been linked to the rising and falling limbs of Milankovitch-driven orbital climate cycles when humidity is neither at a maximum (too wet, siliciclastics dominate) nor a minimum (too dry, evaporation significantly exceeds precipitation) (Ashley, 2007; Ashley et al., 2014). To better understand the climatic conditions that promoted carbonate precipitation in the Calama Basin, more detailed age dating is required, allowing relationships between other climate records and orbital cycles to be made.

This study does, however, show that the Opache lacustrine and palustrine limestones formed during a minimum of 3.5 Ma (K/Ar and Ar-Ar dates obtained from ignimbrites and ashes interbedded with the Opache Formation, May et al., 1999; Blanco and Tomlinson, 2009), when there was relative tectonic quiescence around the Calama Basin,

coupled with a "just right" climate such that sufficient water entered the depositional environment for significant carbonate production, but was insufficient to transport large amounts of siliciclastics material into the basin, which would have overwhelmed carbonate production.

6.2. Basin configuration

This study's GIS-based paleogradient results confirm field and petrographic evidence that the Calama constriction formed a barrier that exerted control on the Opache Formation's sedimentology and stratigraphy. Basin narrowing at the Calama constriction was due to two topographic features; a knob of Eocene strata (the Calama Hill) that formed a partial barrier across the narrow part of the Calama Basin just west of the present city of Calama, and a gap in the Precordillera Highlands where the eastern, N-S oriented Calama Basin became reoriented E-W (Figs. 1, 18). This Late Miocene–Early Pliocene topography, coupled with a very low gradient in the eastern basin (Fig. 6) meant that water ponded east of the constriction and higher gradients to the west meant greater surface water flow velocities there, as shown by sedimentary structures indicating flowing water. As revealed by the GIS-derived cross sections, the eastern part of the Calama Basin has a low area centered at Angostura (Fig. 6). Water accumulated there and covered nearby areas during lake expansion, depositing carbonate north of Chiu-Chiu, and nearly as far west as Calama. The lake's eastern margin, where Opache carbonate interfingers with braidplain and fluvial sediments of the Chiquinaputo Formation, is not seen in outcrop, but Opache limestone is exposed in a 1 km diameter depression (2 km SE of the Río Loa–Río Salado confluence in Pampa Llalqui (SW of an ~1 km diameter doline structure, Fig. 2)), 9 km northeast of Angostura, suggesting that the lake extended at least that far (Fig. 2).

The eastern lacustrine facies formed a gentle gradient, ramp-type margin into the intrabasinal low at Angostura (de Wet et al., 1998; May et al., 1999). Subsidence and compaction created additional accommodation space for groundwater accumulation relative to the western topography, which lacked a central low area. These topographic differences are expressed through the development of different facies, with different diagenetic histories, and different isotopic values, in the resultant limestones. Overall, however, the Opache Formation represents near equilibrium conditions where the generation of accommodation

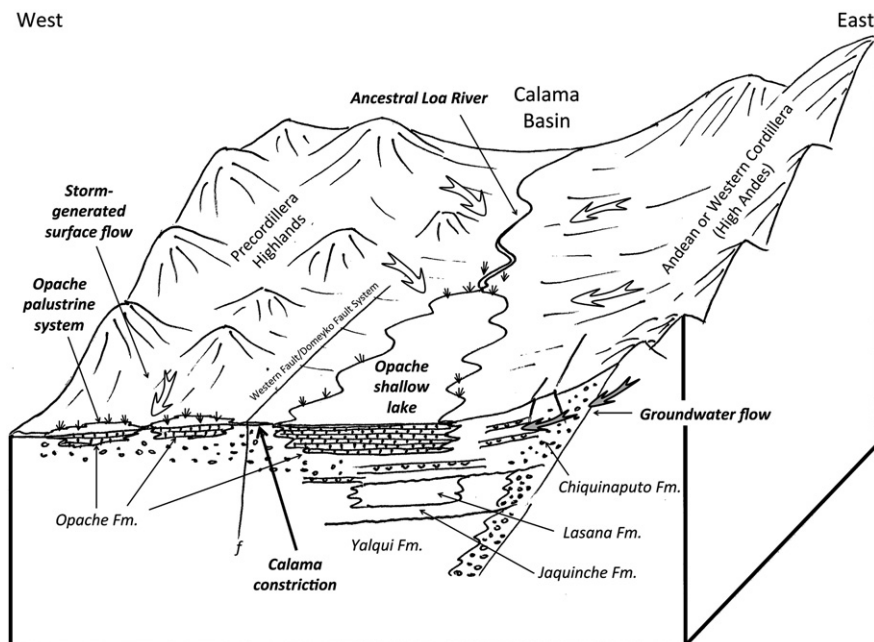


Fig. 18. Reconstruction of Opache Formation paleoenvironments. Arrows indicate groundwater +/– surface water flow from the eastern highlands through underlying and laterally adjacent coarse-grained alluvium, and storm-generated surface runoff from the Precordillera Highlands near the Calama constriction into the western part of the basin.

space kept pace with carbonate accumulation, maintaining shallow water conditions over ~3.5 Ma.

Local topography also influenced siliciclastic sedimentation patterns. Siliciclastic sediment abundance and deposition rates changed from east to west across the Calama Constriction. In the east, siliciclastic grains rarely comprise more than ~20% of the sediment in the lacustrine limestones (excepting the ashfall horizon), but to the west, lithic clasts and mineral grains may constitute 40% or more of the clasts in individual beds, particularly in crossbedded, shallow channel fills. If carbonate precipitation rates from both areas were roughly equivalent, sedimentation rates in the west may have been significantly higher due to the influx of siliciclastic material. Precordillera Highlands are directly adjacent to the Opache depositional basin at the Calama Constriction (~1 km to the north), providing a ready source of material to be washed into the western basin. Alternatively, deformation associated with the Western Fault was hypothesized to have resulted in the siliciclastic-rich limestone west of Calama (May, 1997), although measurement of fault motion suggests that this was unlikely (Tomlinson and Blanco, 1997; Tomlinson et al., 2010). Clasts were probably transported in episodic storm events rather than perennial streams as the grains are angular to subangular, unweathered, and contain abundant lithic fragments, indicating an immature depositional regime (Folk, 1951). The absence of continuous channels or point bar deposits also suggests episodic, rather than perennial, flow conditions.

6.3. Water levels and solute sources

We suggest that rainfall and snowmelt in the mountains to the east and north flowed towards the Calama Basin primarily as groundwater, in combination with rain falling over the Precordillera, produced sufficient freshwater to sustain the Opache lacustrine–palustrine depositional environment for ~3.5 Ma or longer. Lack of evidence for significant fluvial transport of siliciclastic material, relative to the formations stratigraphically below the Opache, which are dominated by alluvial fan clastics, combined with the Opache's overall fine grain size and grain angularity suggests that the amount of surface water entering the lake east of the Calama Constriction was minimal. Instead, water arrived primarily as groundwater, driven by high Andean mountain headwaters, as discussed by Hartley (2007) and transmitted through underlying clastic units. Since evapotranspiration losses are much less from groundwater than surface water, it is possible to transport groundwater long distances without losing it to atmosphere, even in arid to hyperarid settings (Ashley et al., 2013). In addition, as water moves slowly through aquifers, it reacts with the host sediments or rocks, increasing its solute concentrations as it progresses (Shapley et al., 2005; Olago et al., 2009). Groundwater flowing towards the Calama Basin from the adjacent mountains would have encountered soluble ash (volcanic glass and other minerals) derived from the region's active volcanoes (de Silva, 1989), abundant geogenic CO₂ mobilized during volcanism, and immature unconsolidated sediments, reaching supersaturation with respect to calcite (and dolomite), such that mineral precipitation readily occurred when the water reached the basin (Fig. 18), as noted by Decampo (2010) and Ashley et al. (2014) in similar settings. Fig. 18 shows our reconstruction of Opache Formation's paleoenvironments. Arrows indicate groundwater +/– surface water flow from the eastern highlands through underlying and laterally adjacent coarse-grained alluvium, the Chiquinaputo and Lasana Formations primarily. Storm-generated surface runoff from the Precordillera Highlands near the Calama constriction provided water to the western part of the basin, probably in conjunction with minor groundwater flow east-to-west at the Calama constriction.

Spring and groundwater-fed lakes and palustrine settings have been interpreted from Mesozoic and Cenozoic basins (Birney-de Wet and Hubert, 1989; de Wet et al., 1998; Gierlowski-Kordesch and Buchheim, 2003), and numerous studies document shallow, groundwater-fed lake and palustrine systems associated with adjacent highland catchment

areas; Holocene, Central Kenya Rift (Olago et al., 2009), Quaternary of Spain (Alonso-Zarza et al., 2006), Plio-Pleistocene deposits in the Río Grande rift (Mack et al., 2000), and East African rifts (Mount and Cohen, 1984; Ashley and Hay, 2002; Ashley et al., 2013). Recent and Late Pleistocene examples from the Central Andes provide particularly useful details and similarities with the Opache strata (Grosjean et al., 1995; Valero Garcés et al., 2008; Pueyo et al., 2011).

6.4. Diagenetic reactions

Lack of significant outflow in the eastern lake meant that it was sensitive to changing water levels due to increased input (freshening) or evaporation (increased salinity). Fluid–sediment interactions, driven by lake expansion and contraction, phreatic and vadose meteoric watertable fluctuations, and capillary rise driven by evaporation, moved the Opache carbonate sediments in and out of saturated and unsaturated zones with respect to carbonate minerals, silica minerals, and sulfate/halite concentrations, as described in numerous studies of shallow lacustrine to palustrine facies where phreatic to vadose conditions, driven by rising and falling water tables, can produce complex diagenetic fabrics and cement phases (Platt, 1989; Armenteros et al., 1995; Alonso-Zarza et al., 2006), similar to those observed in the Opache Formation's eastern carbonate succession.

This is particularly well expressed through the complex diagenetic history we observed in the lacustrine facies limestones; with multiple generations of calcite cement precipitation (equant and dogtooth spar, inclusion-rich and inclusion-poor phases), dissolution, dolomitization, silicification, and gypsum and halite precipitation. The diagenetic sequence in the eastern limestones shows that phreatic and vadose fluids permeated the upper beds during drying and pedogenesis. Undersaturated fluids dissolved aragonite (leaving gastropod molds), locally reprecipitating carbonate as isopachous sparry cements and/or dolomite. Spötl and Wright (1992) and Bustillo and Alonso-Zarza (2007) describe dolomite formed by water table fluctuations and Colson and Cojan (1996) and Hurwitz et al. (2000) attribute dolomite precipitation in shallow lacustrine strata as the result of lake level fluctuations. In such situations, vertical and horizontal fluid migration mobilizes ions and evaporative concentration results in dolomite precipitation (Armenteros et al., 1995; Arenas et al., 1997). Opache Formation petrography suggests a similar mechanism for both dolomitization and silicification during early diagenesis. Dolomitization in the Opache strata is patchy and aerially restricted, indicating that localized aragonite/calcite dissolution enhanced CaCO₃ concentrations, and Mg, likely sourced from abundant igneous material in the catchment area, or possibly from calcareous spring deposits in the Lasana Formation (Blanco, 2008; Blanco and Tomlinson, 2009), was available for incorporation into authigenic minerals (Olago et al., 2009).

Silicification follows a similar pattern of localized distribution. Often, silicification and carbonate precipitation follow opposite pH trajectories, and their interwoven relationship in the Opache may reflect changing pH in phreatic porewaters, but volcanic glass is geochemically so unstable that it takes only minor fluctuations in porewater chemistry to put it into solution (Hay and Reeder, 1978; McCarthy and Ellery, 1995; Quade et al., 1995). Molds of volcanic glass shards in the Opache limestones indicate that remobilized silica was readily available to precipitate as chert and amorphous silica, as observed petrographically and noted with X-Ray Diffraction.

Diagenesis in the palustrine limestones west of the Calama constriction is not as complex, with less calcite cementation, less dolomitization and less silicification, indicating less diagenetic fluid–sediment interaction. It appears that since the Pliocene, rainfall and groundwater flow has been insufficient to produce any significant diagenetic features, except perhaps some minor gypsum precipitation post-Pliocene (Houston et al., 2008; Amundson et al., 2012). It is also likely that incision by the Ríos Loa and San Salvador quickly left much of the Opache above the water table, and lack of rainfall means that minimal

fluid–sediment diagenetic reactions have occurred since the Late Pliocene (Amundson et al., 2012).

6.5. Isotopic constraints

6.5.1. Strontium

The Sr isotope compositions of the Opache carbonates and modern rivers are consistent with Sr derived from volcanic rocks associated with arc and basement rocks of the Precordillera. The volume of ignimbrites erupted in the Altiplano Puna Volcanic Complex, part of which contributes part of the eastern rim of the Calama Basin highlands, reached about 10^4 km^3 between 10 and 3 Ma ago, with pulses at 8.4 and 4 Ma ago (de Silva and Gosnold, 2007). Regional ignimbrites have $^{87}\text{Sr}/^{86}\text{Sr}$ values between 0.708 and 0.716, and andesites between 0.705 and 0.708 (de Silva et al., 2006; Mattioli et al., 2006; Kay et al., 2010). The Precordillera is geologically complex. Where data exist, these rocks can be very radiogenic but tend to contain little Sr, but perhaps surprisingly, the Cretaceous granites have been found to be unradiogenic (0.705) and have as much as 1000 ppm Sr (Lucassen et al., 1999a,b); possible Jurassic aged marine metasediments within the Precordillera may be an additional source of unradiogenic Sr (Arcuri and Brimhall, 2003). The less radiogenic signature of the Río Loa, relative to the Ríos Salado and San Pedro, appears to be influenced by the runoff from the Precordillera because the Precordillera contains Sr rich, unradiogenic granite.

If we assume the distribution in $^{87}\text{Sr}/^{86}\text{Sr}$ in the modern river system is broadly applicable to the past, the distribution of $^{87}\text{Sr}/^{86}\text{Sr}$ across the Opache Formation is consistent with predominantly arc-sourced water into the lake system east of Calama while water which formed palustrine carbonates west of the Calama Constriction was more heavily influenced by the Precordillera, consistent with the detrital material found in the carbonates (Blanco, 2008). The decrease in $^{87}\text{Sr}/^{86}\text{Sr}$ at the top of the Angostura section suggests a change in the relative contributions of water with a relative decline in water sourced from the east, or more likely, weathering of new sources of unradiogenic Sr such as the embryonic volcanoes of the San Pedro–Linzor volcanic chain (Godoy et al., 2014).

6.5.2. Organic $\delta^{13}\text{C}$

Data for land plants, algae and aquatic vegetation in the Central Andes (Chungara area) show that ^{13}C is enriched in aquatic plants and algae relative to land plants (Pueyo et al., 2011). The highest $\delta^{13}\text{C}_{\text{org}}$ values at Angostura occur 5 m above the base, at 15 m, and at 32.5 m (Fig. 12b). During the times when carbonate fabrics suggest relatively shallow conditions, $\delta^{13}\text{C}_{\text{org}}$ was generally low, consistent with a large component of organic matter derived from plants growing in the littoral zone. As lacustrine conditions became well established (e.g. at 5 and 15 m), there are increases in $\delta^{13}\text{C}_{\text{org}}$, consistent with aquatic plants and algae. The high $\delta^{13}\text{C}_{\text{org}}$ value at 32.5 m may also indicate predominance of aquatic plants and algae. The low $\delta^{13}\text{C}_{\text{org}}$ value at 18.5 m, the height at which a thick siliciclastic ash-bearing unit is present, is interpreted as an indication that littoral zone vegetation was eroded and carried farther into the lake in association with the eruptive event.

6.5.3. Carbonate $\delta^{13}\text{C}$ and $\delta^{18}\text{O}$

The C and O stable isotope compositions are similar to carbonates in the Loa group and to other Pleistocene and Holocene systems in the Central Andes and northern Chile, where the $\delta^{13}\text{C}$ is driven to positive values due to outgassing of CO_2 from carbonate-charged water as it equilibrates with the atmosphere (Grosjean, 1994; Valero Garcés et al., 1999; Rech et al., 2010; Pueyo et al., 2011).

The change in stable isotope composition through the carbonate section at Angostura bears similarities with the pattern of change recorded in the palustrine carbonates to the west of Calama at Quebrada Opache (Rech et al., 2010) (Fig. 12). However, at Quebrada Opache, both $\delta^{13}\text{C}$ and $\delta^{18}\text{O}$ are higher than at Angostura, ranging from +3%

to +7‰ compared to +2‰ to +5‰, and from −4‰ to +1‰ compared to −5.5‰ to −3.2‰. The difference in $\delta^{18}\text{O}$ between the eastern lake and the western palustrine setting ranges from +1 to +4‰, generally increasing up-section. The difference in $\delta^{13}\text{C}$ between the eastern and western carbonates (western data from Rech et al., 2010) is smaller, between 1 and 2‰. The stratigraphic section at Quebrada Opache is about 2 times as thick as at Angostura due to the influx of detrital material, but the somewhat similar pattern of change in both $\delta^{13}\text{C}$ and $\delta^{18}\text{O}$ suggests that carbonates in both locations record the same changes in hydrology.

The covariance between $\delta^{18}\text{O}$ and $\delta^{13}\text{C}$ in Angostura samples only produces an r^2 of 0.26 (Fig. 13). In general, correlation between $\delta^{18}\text{O}$ and $\delta^{13}\text{C}$ occurs during evaporation as water vapor is enriched in ^{18}O , plus increases in temperature and salinity may cause evasion of $^{12}\text{CO}_2$ as CO_2 saturated water equilibrates with the atmosphere. Plotted together, Angostura and Quebrada Opache form a single trend in isotope space ($r^2 = 0.73$; Fig. 13). This is consistent with a groundwater fed lake spilling westward and evaporating as it flowed. However, our petrography shows that diagenetic fabrics are less complex in the western strata compared to the complex paragenesis that characterizes the Angostura section. That the stable isotope compositions at Angostura are not as enriched as those at Ojo Opache is somewhat surprising.

While the minor diagenetic features of the western carbonates, relative to the eastern carbonates, may represent less variable geochemistry than the eastern carbonates were exposed to, and that the water was more saline in the east, paleocurrent directions indicate that siliciclastic material was transported by surface flow from the local upland Precordillera (Blanco, 2008). Groundwater flow from the developing Andean arc fed the eastern lake (Blanco, 2008). For the limestone at Angostura to have indications of more saline conditions, which periodically formed gypsum and even halite, but still have lower $\delta^{18}\text{O}$ than the limestone units to the west, the initial inflowing groundwater from the Andes must have been even more depleted in ^{18}O .

The Angostura lacustrine carbonates have a range of $\delta^{13}\text{C}$ values which are similar to those measured in samples from the underlying Lasana and overlying Chiu–Chiu formations, and a range of $\delta^{18}\text{O}$ values that lie directly on the trend defined by formations stratigraphically below and above the Opache (Rech et al., 2010). If the water from which the Quebrada Opache limestone formed was largely unevaporated, precipitation that fell over the Precordillera had to be more enriched in ^{18}O than precipitation which fell on the Andes and which created the lake system around Angostura. This presents two options, but with similar ramifications. Either meteoric water was sourced from two regions, the Pacific for precipitation falling on the Precordillera and the Atlantic for precipitation falling on the Andes (as it does today, e.g., Aravena et al., 1999), or precipitation which fell on both the Precordillera and the Andes was all sourced from the Pacific and the decrease in $\delta^{18}\text{O}$ simply reflects the rainout effect where water vapor loses ^{18}O to precipitation as it traverses across land (Dansgaard, 1964). Thus, rather than representing a period of hyperaridity caused by Andean uplift (Rech et al., 2010), our petrographic and isotopic studies indicate overall wetter conditions, and importantly, a western source of water to the basin during the deposition of the Opache Formation.

7. Climatic and regional tectonics

The uplift of the Andes during the latter half of the Cenozoic, blocking easterly flow of moist air, has been a factor reducing precipitation on the western side of the Andes, but can uplift account for all of the hydrologic decline of the Atacama region? Garreaud et al. (2010) point out that modeling studies which reduce the height of the Andes do not result in more humid conditions over the Atacama, and the position of the Bolivian High, an area of summer convective activity and rain on the Altiplano and which contributes to the blocking of westward flow moist air over the Andes, is determined by heating over the Amazon

(Lenters and Cook, 1997). The appearance of relatively large groundwater fed lakes at the end of the Miocene through the Middle Pliocene does not seem consistent with uplift creating drier conditions in the Central Andes, though such systems do not necessarily inform us of *local* conditions.

An alternative account for changes in the hydrologic budget addresses global climate. As noted by Sáez et al. (2012), the period over which the Opache carbonates were deposited correlates with a period of time when eastern boundary upwelling such as the Peru–Chile and Benguela systems, which initiated around 10 Ma, had waned in intensity, and warm surface ocean conditions had returned to these areas by the latest Miocene (Siesser, 1980; Ibaraki, 1992, 2001; Abe et al., 2006). The isotopic indications of a Pacific source of moisture during the deposition of the Opache are consistent with a collapse in the temperature inversion which today prevents moisture from being able to cross over the Coastal Cordillera and reach the eastern interior parts of northern Chile. Weakening of this temperature inversion, or warming of the coastal ocean is characteristic of El Niño conditions that brings rainfall to the coastal areas of Northern Chile, but it is also possible that the surface ocean warmed while upwelling persisted if the surface ocean had warmed in high southern latitudes. The final stages of Opache Formation deposition coincide with re-establishment of upwelling of cold water conditions (Ibaraki, 1992, 2001), conclusions similarly reached by Sáez et al. (2012) from stratigraphic relationships between the Calama and west neighboring Quillagua–Llamara Basin.

8. Conclusions

By the Late Miocene the Andes had attained significant physiographic relief, but there was insufficient rainfall to transport coarse-grained siliciclastic material out into the center of the Calama Basin, as evidenced by the change from alluvium-dominated deposition to carbonate (Opache Formation) within the El Loa Group. A topographic low in the basin accumulated limestone, produced by CO₂-charged groundwater derived from the mountains to the east. Interpretation of the Opache Formation's bioturbated, non-laminated, light-colored, lacustrine and palustrine facies indicates a non-stagnant, non-stratified, freshwater setting, supersaturated with respect to carbonate. The lacustrine and palustrine facies differ in terms of water depth, the energy of water flow, and water sources (Fig. 18). For example, the lacustrine facies, well exposed at Angostura, consists of at least 35 m of limestone and silty-sandy micrite with a small detrital fraction of silt and sand sized siliciclastic grains (except the ash beds), unabraded ostracods and diatoms, and delicate ash shards, suggesting a calm lacustrine environment with consistent water cover (except for the lowermost 2 m and uppermost 4.25 m). In contrast, palustrine facies limestones occur predominantly west of the Calama constriction and are dominated by oncrites, gastropods, stromatolites, ooids, and crossbedded detrital material up to gravel size, indicating flowing water. Evidence for repeated exposure and pedogenesis includes mudcracks, circumgranular cracks, root traces, vuggy and fenestral pores, fossil molds, meniscus and pendant cements, and Mn dendrites.

Palustrine carbonates on the western side of the Calama Constriction formed from a mixture of water sourced in the nearby Precordillera highlands and mineralized water which seeped from the eastern lake system. Precipitation in the Precordillera initiated episodic flood events which transported clasts up to gravel size into the palustrine environment, but did not transport coarse siliciclastics into the eastern system due to distance from the source area.

Terrestrial carbonates are very sensitive to precipitation changes, therefore, precipitation increases in the Andean highlands resulted in lake expansion, followed by contraction and evaporative concentration of porewaters, inducing evaporate mineral precipitation. The Calama Basin was closed, with no outlet to the sea, and therefore, could be subject to significant evaporation, as evidenced by gypsum, anhydrite, and minor halite precipitation. When the groundwater flow rate

exceeded the evaporation rate, lacustrine to palustrine facies were deposited.

Igneous rock fragments and fresh mineral grains are abundant throughout the Opache Formation, but may constitute >40% of the clasts in some of the western strata, indicating local sources without deep weathering. This supports the interpretation that the climate was already *at least* semi-arid during Opache depositional time, but the occurrence of coarse-grained, cross bedded, detrital lenses suggests that significant flash flood-type events episodically washed in clasts from the adjacent Precordillera highlands.

The diagenetic sequence in the eastern Opache limestones is more complex than in the western facies because the waters were rich in dissolved ions due to their groundwater origin, and changing lake levels and water table conditions around the lake margin drove diagenetic reactions, such as volcanic glass and aragonite dissolution, gypsum and halite precipitation, dolomitization, and silicification. In the west, surface water flow from Precordillera rainfall, coupled with frequent subaerial exposure associated with palustrine shallows meant that there was less water available, with shorter residence time, to drive significant post-depositional diagenetic change.

Srontium isotope results indicate that much of the groundwater feeding the lake was derived from the eastern highlands (arc terrain), but that a less radiogenic source, probably derived from Sr-rich, Rb-poor granite in the Precordillera entered and was incorporated into the carbonates in the west. Although carbonates in the east show more influence of evaporation, their stable isotope composition is less enriched in ¹⁸O than the palustrine carbonate to the west, implying that water which fell in the Andes had much lower $\delta^{18}\text{O}$ than rain which fell in the west.

Our findings suggest that Opache deposition occurred during a period of increased, but episodic, rainfall, coupled with a period of increased groundwater flow, sourced from the Andean highlands to the east. The indications of increased rainfall over the Precordillera are consistent with Pacific-sourced moisture, as suggested by stable isotope measurements, linked to warmer sea surface temperatures.

Acknowledgments

Funding was provided by the National Science Foundation (EAR-1117496) to LG, with additional funds from Franklin & Marshall College to CdW. Thank you to S. Sylvester and Chi Xu for analytical assistance and S. Gigliotti for help with the figures. We would particularly like to acknowledge John Houston for highlighting the Opache as a unique system of paleoenvironmental interest, as well as Teresa Jordan (Cornell University), and Nicolas Blanco and Andy Tomlinson (Serageomin) for very useful and informative discussions. Stable isotope analyses were made with the assistance of James Wright and Rick Mortlock at Rutgers University. We thank the manuscript reviewers for their comments and suggestions that improved the paper.

Appendix A. Supplementary data

Supplementary data associated with this article can be found in the online version, at <http://dx.doi.org/10.1016/j.palaeo.2015.02.039>. These data include Google map of the most important areas described in this article.

References

- Abe, C., Yamamoto, M., Irino, T., 2006. Data report: organic carbon and biomarker variations, Sites 1237 and 1239. In: Tiedemann, R., Mix, A.C., Blum, P., Ruddiman, W.F. (Eds.), Proceedings of the Ocean Drilling Program, Scientific Results, 202. Ocean Drilling Program, College Station, TX, pp. 1–14.
- Alonso-Zarza, A.M., 2003. Palaeoenvironmental significance of palustrine carbonates and calcretes in the geological record. *Earth Sci. Rev.* 60, 261–298.
- Alonso-Zarza, A.M., Dorado-Valiño, M., Valdeolmillos-Rodríguez, A., Ruis-Zapata, M.B., 2006. A recent analogue of palustrine carbonate environments: the Quaternary

- deposits of Las Tablas de Daimiel wetlands, Ciudad Real, Spain. *GSA Spec. Paper* 416 pp. 153–168.
- Alonso-Zarza, A.M., Meléndez, A., Martín García, R., Herrero, M.J., Martín-Pérez, A., 2012. Discriminating between tectonism and climate signatures in palustrine deposits: lessons from the Miocene of the Teruel Graben, NE Spain. *Earth-Sci. Rev.* 113, 141–160.
- Alpers, C.N., Brimhall, G.H., 1988. Middle Miocene climatic change in the Atacama Desert, northern Chile: evidence from supergene mineralization at La Escondida. *Geol. Soc. Am. Bull.* 100, 1640–1656.
- Amundson, R., Dietrich, W., Bellugi, D., Ewing, S., Nishiizumi, K., Chong, G., Owen, J., Finkel, R., Heimsath, A., Stewart, B., Caffee, M., 2012. Geomorphologic evidence for the late Pliocene onset of hyperaridity in the Atacama Desert. *Geol. Soc. Am. Bull.* 124, 1048–1070.
- Andrews, J.E., Coletta, P., Pentecost, A., Riding, R., Dennis, S., Dennis, P.F., Spiro, B., 2004. Equilibrium and disequilibrium stable isotope effects in modern *Charophyte* calcites: implications for palaeoenvironmental studies. *Palaeogeogr. Palaeoclimatol. Palaeoecol.* 204, 101–114.
- Arakel, A.V., Hongjun, T., 1994. Seasonal evaporate sedimentation in desert playa lakes of the Karinga Creek drainage system, Central Australia. In: Renaut, R.W., Last, W.M. (Eds.), *Sedimentology and Geochemistry of Modern and Ancient Saline Lakes*. Society for Sedimentary Geology, Tulsa, pp. 91–100.
- Aravena, R., Suzuki, O., Peña, H., Pollastri, A., Fuenzalida, H., Grilli, A., 1999. Isotopic composition of the precipitation in Northern Chile. *Appl. Geochem.* 14, 411–422.
- Arcuri, T., Brimhall, G.H., 2003. The chloride source for atacamite mineralization at the Radomiro Tomic porphyry copper deposit, northern Chile. *Econ. Geol.* 98, 1667–1681.
- Arenas, C., Casanova, J., Pando, G., 1997. Stable isotope characterization of the Miocene lacustrine systems of Los Monegros (Ebro Basin, Spain): palaeogeographic and palaeoclimatic implications. *Palaeogeogr. Palaeoclimatol. Palaeoecol.* 128, 133–155.
- Armenteros, I., Angeles Bastillo, M.A., Blanco, J.A., 1995. Pedogenic and groundwater processes in a closed Miocene basin (northern Spain). *Sediment. Geol.* 99, 17–36.
- Ashley, G.M., 2007. Orbital rhythms, monsoons, and playa lake response, Olduvai Basin, equatorial East Africa (ca. 1.85–1.74 Ma). *Geol. Soc. Am. Bull.* 35, 1091–1094.
- Ashley, G.M., Hay, R., 2002. Sedimentation patterns in a Plio-Pleistocene volcaniclastic rift-platform basin, Olduvai Gorge, Tanzania. *Sedimentation in Continental Rifts*. SEPM Spec. Pub No. 73. *Sedimentation in Continental Rifts*, Tulsa, pp. 107–122.
- Ashley, G.M., Tactikos, J.C., Owen, R.B., 2009. Hominin use of springs and wetlands: paleoclimate and archeological records from Olduvai Gorge (~1.79–1.74 Ma). *Palaeogeogr. Palaeoclimatol. Palaeoecol.* 272, 1–16.
- Ashley, G.M., Deocampo, D.M., Kahmann-Robinson, J., Driese, S.G., 2013. Groundwater-fed wetland sediments and paleosols: it's all about the water table, new frontiers in paleopedology and terrestrial paleoclimatology: paleosols and soil surface analog systems. *SEPM Special Publication No. 11*, pp. 47–61.
- Ashley, G.M., de Wet, C.B., Dominguez-Rodrigo, M., Karis, A.M., O'Reilly, T.M., Baluyot, R., 2014. Freshwater limestone in an arid rift basin: a goldilocks effect. *J. Sediment. Res.* 84, 988–1004.
- Bathurst, R.G.C., 1975. *Carbonate Sediments and Their Diagenesis*. Elsevier, Amsterdam (658 pp.).
- Bird, B.W., 2009. Tropical climate records from small Andean Lakes. *GSA Limnogeology Division Newsletter* vol. 7, no. 1 pp. 8–12.
- Binney-de Wet, C., Hubert, J.H., 1989. The Scots Bay Formation, Nova Scotia, Canada: a Jurassic lake with silica-rich hydrothermal springs. *Sedimentology* 36, 857–874.
- Blanco, N., 2008. *Estratigrafía y evolución tectono-sedimentaria de la cuenca cenozoica de Calama (Chile, 22°S)*. (M.S. Thesis), University of Barcelona (68 pp. (Spanish)).
- Blanco, N., Tomlinson, A., 2009. Carta Chiu Chiu, Región de Antofagasta. Servicio Nacional de Geología y Minería, Carta Geológica de Chile, Series Basic Geology, Scale 1:50.000. Santiago, 26 pp.
- Bohacs, K.M., Grabowski Jr., G., Carroll, A.R., 2007. Lithofacies architecture and variation in expression of sequence stratigraphy within representative intervals of the Green River Formation, Greater Green River Basin, Wyoming. *Mt. Geol.* 44, 39–58.
- Burne, R.V., Bauld, J., DeDeckker, P., 1980. Saline lake *Charophytes* and their geological significance. *J. Sediment. Petrol.* 50, 281–293.
- Bustillo, M.A., Alonso-Zarza, A.M., 2007. Overlapping of pedogenesis and meteoric diagenesis in distal alluvial and shallow lacustrine deposits in the Madrid Basin, Spain. *Sedimentol. Geol.* 198, 255–271.
- Cabaleri, N.G., Benavente, C.A., 2013. Sedimentology and paleoenvironments of the Las Charitas carbonate paleolake, Cañadón Asfalto Formation (Jurassic), Patagonia, Argentina. *Sediment. Geol.* 284–285, 91–105.
- Cañaveras, J.C., Sánchez-Moral, S., Calvo, J.P., Hoyos, M., Ordóñez, S., 1996. Dedolomites associated with karstification, an example of early dedolomitization in lacustrine sequences from the Tertiary Madrid Basin, Central Spain. *Carbonates Evaporites* 11, 85–103.
- Casanova, J., 1986. East African rift stromatolites. In: Frostick, L.E., Renaut, R.W., Reid, I., Tiercelin, J.J. (Eds.), *Sedimentation in the African Rifts*. Geological Society Special Publication No. 25. Blackwell, pp. 201–210.
- Casanova, J., 1994. Stromatolites from the East African rift: a synopsis. In: Bertrand-Sarfati, J., Monty, C. (Eds.), *Phanerozoic Stromatolites II*. Kluwer Academic Pub, Dordrecht, pp. 193–226.
- Cecil, C.B., 1990. Paleoclimate controls on stratigraphic repetition of chemical and siliciclastic rocks. *Geology* 18, 533–536.
- Chafetz, H.S., Guidry, S.A., 2003. Deposition and diagenesis of Mammoth Hot Springs travertine, Yellowstone National Park, Wyoming, USA. *Can. J. Earth Sci.* 40, 1515–1529.
- Chong, G., Mendoza, M., García-Veigas, Pueyo, J.J., and Turner, P., 1999. Evolution and geochemical signatures in a Neogene forearc evaporitic basin: the Salar Grande (Central Andes of Chile). *Palaeogeogr. Palaeoclimatol. Palaeoecol.* 151, 39–54.
- Colson, J., Cojan, I., 1996. Groundwater dolocretes in a lake-marginal environment: an alternative model for dolocrete formation in continental settings (Danian of the Provence Basin, France). *Sedimentology* 43, 175–188.
- Coshell, L., Rosen, M.R., 1994. Stratigraphy and Holocene history of Lake Hayward, Swan coastal plain wetlands, Western Australia. In: Renaut, R.W., Last, W.M. (Eds.), *Sedimentology and Geochemistry of Modern and Ancient Saline Lakes*. Society for Sedimentary Geology, Tulsa, pp. 173–188.
- Dansgaard, W., 1964. Stable isotopes in precipitation. *Tellus* 16, 436–468.
- de Silva, S.L., 1989. Geochronology and stratigraphy of the ignimbrites from the 21° 30'S to 23° 30'S portion of the Central Andes of northern Chile. *J. Volcanol. Geotherm. Res.* 37, 93–131.
- de Silva, S., Gosnold, W.D., 2007. Episodic construction of batholiths: insights from the spatiotemporal development of an ignimbrite flare-up. *J. Volcanol. Geotherm. Res.* 167, 320–325.
- de Silva, S., Zandt, G., Trumbull, R., Viramonte, J.G., Salas, G., Jiménez, N., 2006. Large ignimbrite eruptions and volcano-tectonic depressions in the Central Andes: a thermomechanical perspective. In: Troise, C., De Natale, G., Kilburn, C.R.J. (Eds.), *Mechanisms of Activity and Unrest at Large Calderas*. Special Publications 269. Geological Society, London, pp. 47–63.
- de Wet, C.B., Yocom, D.A., Mora, C.I., 1998. Carbonate lakes in closed basins: sensitive indicators of climate and tectonics; an example from the Gettysburg Basin (Triassic), Pennsylvania, USA. In: Shanley, K., McCabe, P. (Eds.), *Relative Role of Eustacy, Climate and Tectonism in Continental Rocks*. SEPM Spec. Pub No. 59, pp. 191–209 (Tulsa).
- de Wet, C.B., Godfrey, L., de Wet, A., 2012. Miocene–Pliocene tufas and palustrine limestones, Opache Fm., Atacama Desert, Chile. *Geological Society of America Abstracts with Program* vol. 44, No. 2 p. 57.
- Dean, W.E., Fouch, T.D., 1983. Lacustrine environment. In: Scholle, P.A., Bebout, D.G., Moore, C.H. (Eds.), *Carbonate Depositional Environments*. American Association of Petroleum Geologists Memoir 33. AAPG, Tulsa, OK, pp. 98–130.
- Decampo, D.M., 2010. The geochemistry of continental carbonates. In: Alonso-Zarza, A.M., Tanner, L.H. (Eds.), *Carbonates in Continental Settings: Geochemistry, Diagenesis and Applications. Developments in Sedimentology* vol. 62. Elsevier, Amsterdam, pp. 1–59.
- Del Cura, M., Calvo, J., Ordóñez, S., Jones, B., Cañaveras, J., 2001. Petrographic and geochemical evidence for the formation of primary, bacterially induced lacustrine dolomite: La Roda 'White Earth' (Pliocene, Central Spain). *Sedimentology* 48, 897–915.
- Dickson, J.A.D., 1966. Carbonate identification and genesis as revealed by staining. *J. Sediment. Petrol.* 36, 491–505.
- Esteban, M., Klappa, C.F., 1983. Subaerial exposure environment. In: Scholle, P.A., Bebout, D.G., Moore, C.H. (Eds.), *Carbonate Depositional Environments*. AAPG, Tulsa, pp. 2–95.
- Folk, R.F., 1951. Stages of textural maturity. *J. Sedimentol. Petrol.* 21, 127–130.
- Freytet, P., Plaziat, J.-C., 1982. Continental carbonate sedimentation and pedogenesis – Late Cretaceous and Early Tertiary of Southern France. In: Purser, B. (Ed.), *Contribution to Sedimentology # 12*. E. Schweizerbart'sche Verlagsbuchhandlung, Stuttgart (213 pp.).
- Freytet, P., Plet, A., 1996. Modern freshwater microbial carbonates: the *Phormidium* stromatolites (Tufa-Travertine) of southeastern Burgundy (Paris Basin, France). *Facies* 34, 219–238.
- Freytet, P., Verrecchia, E.P., 2002. Lacustrine and palustrine carbonate petrography: an overview. *J. Paleolimnol.* 27, 221–237.
- Garreaud, R.D., Molina, A., Farias, M., 2010. Andean uplift, ocean cooling and Atacama hyperaridity: a climate modeling perspective. *Earth Planet. Sci. Lett.* 292, 39–50.
- Garzione, C.N., Hoke, G.D., Libarkin, J.C., Withers, S., MacFadden, B., Eiler, J., Ghosh, P., Mulch, A., 2008. Rise of the Andes. *Science* 320, 1304–1307.
- Gierlowski-Kordesch, E.H., 1998. Carbonate deposition in an ephemeral siliciclastic alluvial system: Jurassic Shuttle Meadow Formation, Newark Supergroup, Hartford Basin, USA. *Palaeogeogr. Palaeoclimatol. Palaeoecol.* 140, 161–184.
- Gierlowski-Kordesch, E.H., Buchheim, H.P., 2003. Lake basins as archives of continental tectonics and paleoclimate: introduction. *J. Paleolimnol.* 30, 113–114.
- Godoy, B., Wörner, G., Kojima, S., Aguilera, F., Simon, K., Hartmann, G., 2014. Low-pressure evolution of arc magmas in thickened crust: the San Pedro-Linzor volcanic chain, Central Andes, Northern Chile. *J. S. Am. Earth Sci.* 52, 24–42.
- Golubic, S., 1991. Modern stromatolites: a review. In: Riding, R. (Ed.), *Calcareous Algae and Stromatolites*. Springer-Verlag, Berlin, pp. 541–561.
- Grosjean, M., 1994. Paleohydrology of the Laguna Lejía (north Chilean Altiplano) and climatic implications for late glacial times. *Palaeogeogr. Palaeoclimatol. Palaeoecol.* 109, 89–100.
- Grosjean, M., Geyh, M.A., Messerli, B., Schotterer, U., 1995. Late-glacial and early Holocene lake sediments, groundwater formation and climate in the Atacama Altiplano 22–24° S. *J. Paleolimnol.* 14, 241–252.
- Hartley, A.J., Chong, G., 2002. A late Pliocene age for the Atacama Desert: Implications for the desertification of western South America. *Geology* 30, 43–46. [http://dx.doi.org/10.1130/0091-7613\(2002\)030<043:lpafa>2.0.CO;2](http://dx.doi.org/10.1130/0091-7613(2002)030<043:lpafa>2.0.CO;2).
- Hartley, A.J., 2007. Neogene climate change and uplift in the Atacama Desert, Chile: comment. *Geology* e120–e121 <http://dx.doi.org/10.1130/G23709C.1>.
- Hartley, A.J., Evenstar, L., 2010. Cenozoic stratigraphic development in the north Chilean forearc: implications for basin development and uplift history of the Central Andean margin. *Tectonophysics* 495, 67–77.
- Hay, R.L., Kyser, T.K., 2001. Chemical sedimentology and paleoenvironmental history of Lake Olduvai, a Pleistocene lake in northern Tanzania. *Geol. Soc. Am. Bull.* 113, 1505–1521.
- Hay, R.L., Reeder, R.J., 1978. Calcrites of Olduvai Gorge and the Ndolanga Beds of northern Tanzania. *Sedimentology* 25, 649–673.
- Hay, R.L., Paxton, R.E., Teague, T.T., Kyser, T.K., 1986. Spring-related carbonate rocks, Mg-clays and associated mineral in Pliocene deposits of the Amargosa Desert, Nevada and California. *GSA Bull.* 97, 1488–1503.
- Hoke, G.D., 2006. The Influence of Climate and Tectonics on the Geomorphology of the Western Slope of the Central Andes, Chile and Peru. (Ph.D. thesis), Cornell Univ, Ithaca, N.Y (283 pp.).

- Houston, J., Hart, D., Houston, A., 2008. Neogene sedimentary deformation in the Chilean forearc and implications for Andean basin development, seismicity and uplift. *J. Geol. Soc. Lond.* 165, 291–306.
- Hurwitz, S., Stanislavsky, E., Lyankovsky, V., Gvirtzman, H., 2000. Transient groundwater–lake interaction in a continental rift: Sea of Galilee Israel. *Geol. Soc. Am. Bull.* 112, 1694–1702.
- Ibaraki, M., 1992. Geologic age of biosiliceous sediments in Peru and Chile based on planktonic foraminifera. *Rev. Geol. Chile* 19, 61–66.
- Ibaraki, M., 2001. Neogene planktonic foraminifera of the Caleta Herradura de Mejillones section in northern Chile: biostratigraphy and paleoceanographic implications. *Micropaleontology* 47, 257–267.
- Johnson, R., Ashley, G.M., de Wet, C.B., Dvorsky, R., Park, L., Hover, V.C., Owen, R.B., McBreaty, S., 2009. Tufas a record of perennial freshwater in a semi-arid rift basin, Kapthurin Formation, Central Kenya. *Sedimentology* 56, 1115–1137.
- Jordan, T.E., Mpodozis, C., Muñoz, N., Blanco, N., Pananont, P., Gardeweg, M., 2007. Cenozoic subsurface stratigraphy and structure of the Salar de Atacama Basin, northern Chile. *J. S. Am. Earth Sci.* 23, 122–146.
- Jordan, T.E., Nester, P.L., Blanco, N., Hoke, G.D., Dávila, F., Tomlinson, A.J., 2010. Uplift of the Altiplano-Puna plateau: a view from the west. *Tectonics* 29, TC5007. <http://dx.doi.org/10.1029/2010TC002661>.
- Kay, S.M., Coira, B.L., Caffé, P.J., Chen, C.-H., 2010. Regional chemical diversity, crustal and mantle sources and evolution of central Andean Puna plateau ignimbrites. *J. Volcanol. Geotherm. Res.* 198, 81–111.
- Lamb, S., Hoke, L., Kennan, L., Dewey, J., 1997. Cenozoic evolution of the central Andes in Bolivia and northern Chile. In: Burg, J.-P., Ford, M. (Eds.), *Orogeny Through Time*. Geological Society Special Publication No. 121, pp. 237–264.
- Lenters, J., Cook, K., 1997. On the origin of the Bolivian high and related circulation features of the South American climate. *J. Atmos. Sci.* 54 (5), 656–678.
- Liutkus, C.M., Ashley, G.M., 2003. Facies model of a semiarid freshwater wetland, Olduvai Gorge, Tanzania. *J. Sediment. Res.* 73, 691–705.
- Lucassen, F., Franz, G., Laber, A., 1999a. Permian high pressure rocks, the basement of the Sierra de Límo Verde in northern Chile. *J. S. Am. Earth Sci.* 12, 183–199.
- Lucassen, F., Franz, G., Thirlwall, M., Mezger, K., 1999b. Crustal recycling of metamorphic basement: Late Palaeozoic granitoids of northern Chile (~22°S), implications for the composition of the Andean crust. *J. Petrol.* 40, 1527–1551.
- Mack, G.H., Cole, D.R., Trevino, L., 2000. The distribution and discrimination of shallow, authigenic carbonate in the Pliocene–Pleistocene Palomas Basin, southern Río Grande rift. *GSA Bull.* 112, 643–656.
- Mack, G.H., Jones, M.C., Tabor, N.J., Ramos, F.C., Scott, S.R., Witcher, J.C., 2012. Mixed geo-thermal and shallow meteoric origin of opal and calcite beds in Pliocene–Lower Pleistocene axial-fluvial strata, Southern Río Grande Rift, Rincon Hills, New Mexico, USA. *J. Sediment. Res.* 82, 616–631.
- Mattioli, M., Renzulli, A., Menna, M., Holm, P., 2006. Rapid ascent and contamination of magmas through the thick crust of the CVZ (Andes, Ollague region): evidence from a nearly aphyric high-K andesite with skeletal olivines. *J. Volcanol. Geotherm. Res.* 158, 87–105.
- May, G., 1997. Oligocene to recent evolution of the Calama Basin, Northern Chile. Thesis, University of Aberdeen (unpubl.), 274 pp.
- May, G., Hartley, A.J., Stuart, F.M., Chong, G., 1999. Tectonic signatures in arid continental basins: an example from the Upper Miocene–Pleistocene, Calama Basin, Andean Forearc, northern Chile. *Palaeogeogr. Palaeoclimatol. Palaeoecol.* 5, 55–77.
- May, G., Hartley, A.J., Chong, G., Stuart, F.M., Turner, P., Kape, S.J., 2005. Eocene to Pleistocene lithostratigraphy, chronostratigraphy and tectono-sedimentary evolution of the Calama Basin, northern Chile. *Rev. Geol. Chile* 32, 33–58.
- McCarthy, T.S., Ellery, W.N., 1995. Sedimentation on the distal reaches of the Okavango fan, Botswana, and its bearing on calcrete and silcrete (ganister) formation. *J. Sediment. Res.* 65, 77–90.
- MDA Federal, 2004. Landsat Geocover ETM + 2000 Edition Mosaics Tile S-19-20. ETM-EarthSat-MrsID, 1.9, USGS, Sioux Falls, South Dakota, 2000.
- Monty, C.L.V., Hardie, L.A., 1972. The geological significance of the freshwater Blue-green algal calcareous marsh. In: Walter, M.R. (Ed.), *Stromatolites*. Elsevier, NY, pp. 447–477.
- Mount, J.F., Cohen, A.S., 1984. Petrology and geochemistry of rhizoliths from Plio-Pleistocene fluvial and marginal lacustrine deposits, East Lake, Turkana, Kenya. *J. Sediment. Petrol.* 54, 263–275.
- Nester, P.L., Gayó, E., Latorre, C., Jordan, T.E., Blanco, N., 2007. Perennial stream discharge in the hyperarid Atacama Desert of northern Chile during the latest Pleistocene. *Proc. Natl. Acad. Sci. U. S. A.* 104, 19, 724–19,729. <http://dx.doi.org/10.1073/pnas.0705373104>.
- Newton, M.S., 1994. Holocene fluctuations of Mono Lake, California: the sedimentary record. In: Renaut, R.W., Last, W.M. (Eds.), *Sedimentology and Geochemistry of Modern and Ancient Saline Lakes*. Society for Sedimentary Geology, Tulsa, pp. 143–157.
- Nickel, E., 1983. Environmental significance of freshwater oncoids, Eocene Guarga Formation, Southern Pyrenees, Spain. In: Peryt, T. (Ed.), *Coated Grains*. Springer-Verlag, Berlin Heidelberg, pp. 308–329.
- Olago, D., Opere, A., Barongo, J., 2009. Holocene palaeohydrology, groundwater and climate change in the lake basins of the Central Kenya Rift. *J. Hydrol. Sci.* 54, 765–780.
- Pananont, P., Mpodozis, C., Blanco, N., Jordan, T.E., Brown, L.D., 2004. Cenozoic evolution of the northwestern Salar de Atacama Basin, northern Chile. *Tectonics* 23, TC6007. <http://dx.doi.org/10.1029/2003TC001595>.
- Peck, R., 1953. Fossil Charophytes. *Bot. Rev.* 19, 209–227.
- Peck, R., 1957. North American Mesozoic Charophytes. USGS Professional Paper 294-A pp. 1–60.
- Pedley, M., Andrews, J., Ordóñez, S., García del Cura, M., González Martín, J.-A., Taylor, D., 1996. Does climate control the morphological fabric of freshwater carbonates? A comparative study of Holocene barrage tufts from Spain and Britain. *Palaeogeogr. Palaeoclimatol. Palaeoecol.* 121, 239–257.
- Pentecost, A., 2005. Travertine. Springer-Verlag, Berlin, Heidelberg (445 pp.).
- Pentecost, A., Andrews, J.E., Dennis, P.F., Marca-Bell, A., Dennis, S., 2006. *Charophyte* growth in small temperate water bodies: extreme isotopic disequilibrium and implications for the palaeoecology of shallow marl lakes. *Palaeogeogr. Palaeoclimatol. Palaeoecol.* 240, 389–404.
- Pla-Pueyo, S., Gierlowski-Kordesch, E.H., Viseras, C., Soria, J.M., 2009. Major controls on sedimentation during the evolution of a continental basin: Pliocene–Pleistocene of the Guadix Basin (Betic Cordillera, southern Spain). *Sediment. Geol.* 219, 97–114.
- Platt, N.H., 1989. Lacustrine carbonates and pedogenesis: sedimentology and origin of palustrine deposits from the Early Cretaceous Rupelo Formation, W. Cameros Basin, N. Spain. *Sedimentology* 36, 665–684.
- Pueyo, J.J., Chong, G., Jensen, A., 2001. Neogene evaporites in desert volcanic environments: Atacama Desert, northern Chile. *Sedimentology* 48, 1411–1431.
- Pueyo, J.J., Sáez, A., Giralt, S., Valero Garcés, B.L., Moreno, A., Bao, R., Schwab, A., Herrera, C., Kłosowska, B., Taberner, C., 2011. Carbonate and organic matter sedimentation and isotopic signatures in Lake Chungará, Chilean Altiplano, during the last 12.3 kyr. *Palaeogeogr. Palaeoclimatol. Palaeoecol.* 307, 339–355.
- Purvis, K., Wright, V.P., 1991. Calcrites related to phreatophytic vegetation from the Middle Triassic Otter Sandstone of southwest England. *Sedimentology* 38, 539–551.
- Quade, J., Chivas, A.R., McCulloch, M.T., 1995. Strontium and carbon isotope tracers and the origins of soil carbonate in South Australia and Victoria. *Palaeogeogr. Palaeoclimatol. Palaeoecol.* 113, 103–117.
- Rech, J.A., Currie, B.S., Michalski, G., Cowan, A.M., 2006. Neogene climate change and uplift in the Atacama Desert, Chile. *Geology* 34, 761–764. <http://dx.doi.org/10.1130/G22444.1>.
- Rech, J.A., Currie, B.S., Shullenberger, E.D., Dunagean, S.P., Jordan, T.E., Blanco, N., Tomlinson, A.J., Rowe, H.D., Houston, J., 2010. Evidence for the development of the Andean rain shadow from a Neogene isotopic record in the Atacama Desert, Chile. *Earth Planet. Sci. Lett.* 292, 371–382.
- Reich, M., Palacios, C., Vargas, G., Luo, S., Cameron, E.M., Leybourne, M.I., Parada, M.A., Zúñiga, A., You, C.-F., 2009. Supergene enrichment of copper deposits since the onset of modern hyperaridity in the Atacama Desert, Chile. *Mineral. Deposita* 44, 497–504.
- Rouchy, J.M., Camoin, G., Casanova, J., Deconinck, J.F., 1993. The Central palaeo-Andean basin of Bolivia (Potosí area) during the late Cretaceous and early Tertiary: reconstruction of ancient saline lakes using sedimentological, paleoecological, and stable isotope records. *Palaeogeogr. Palaeoclimatol. Palaeoecol.* 105, 179–198.
- Sáez, A., Cabrera, L., Jensen, A., Chong, G., 1999. Late Neogene lacustrine record and paleogeography in the Quillagua–Llamara Basin, Central Andean Fore-arc (northern Chile). *Palaeogeogr. Palaeoclimatol. Palaeoecol.* 151, 5–37.
- Sáez, A., Cabrera, L., Garcé, M., van den Bogaard, P., Jensen, A., Gimeno, D., 2012. The stratigraphic record of changing hyperaridity in the Atacama Desert over the last 10 Ma. *Earth Planet. Sci. Lett.* 355–356, 32–38.
- Shapley, M.D., Ito, E., Donovan, J.J., 2005. Authigenic calcium carbonate flux in groundwater-controlled lakes: implications for lacustrine paleoclimate records. *Geochim. Cosmochim. Acta* 69, 2517–2533.
- Siesser, W.G., 1980. Late Miocene origin of the Benguela upswelling system off northern Namibia. *Science* 208, 283–285.
- Spötl, C., Wright, V.P., 1992. Groundwater dolocretes from the Upper Triassic of the Paris Basin, France: a case study of an arid, continental diagenetic facies. *Sedimentology* 39, 1119–1137.
- Tomlinson, A., Blanco, N., 1997. Structural evolution and displacement history of the West Fault System, Precordillera, Chile: part 2, postmineral history: Congreso Geológico Chileno, 8 (3), 1878–1882.
- Tomlinson, A.J., Blanco, N., Dilles, J.H., 2010. Carta Calama, Región de Antofagasta: Carta Geológica de Chile, SERNAGEOMIN Serie Preliminar No. 8. Subdirección Nacional de Geología, Santiago, Chile.
- Valdeolmillos-Rodríguez, A., Dorado-Valiño, M., Ruiz-Zapata, M.B., Alonso-Zarza, A.M., 2011. Middle Pleistocene variations in palaeoclimate, palaeoenvironment and vegetation of the Las Tablas de Daimiel National Park (Spain). *J. Quat. Sci.* 26 (1), 128–140.
- Valero Garcés, B.L., Delgado-Huertas, A., Ratto, N., Navas, A., 1999. Large ^{13}C enrichment in primary carbonates from Andean Altiplano lakes, northwest Argentina. *Earth Planet. Sci. Lett.* 171, 253–266.
- Valero Garcés, B.L., Moreno, A., Navas, A., Mata, P., Machin, J., Delgado Huertas, A., González Samperiz, P., Schwab, A., Merrellon, M., Cheng, H., Edwards, R.L., 2008. The Taravilla lake and tufa deposits (Central Iberian Range, Spain) as palaeohydrological and paleoclimatic indicators. *Palaeogeogr. Palaeoclimatol. Palaeoecol.* 259, 136–156.
- Vázquez-Urbex, M., Arenas, C., Pardo, G., 2012. A sedimentary facies model for stepped, fluvial tufa systems in the Iberian Range (Spain): the Quaternary Piedra and Mesa Valleys. *Sedimentology* 59, 502–526.
- Wetzel, R.G., 1983. *Limnology*. Saunders College Publishing, Philadelphia (110 pp.).
- Wright, V.P., Tucker, M.E. (Eds.), 1991. *Calcretes*. International Association of Sedimentologists Reprint Series vol. 2. Blackwell, Oxford (352 pp.).